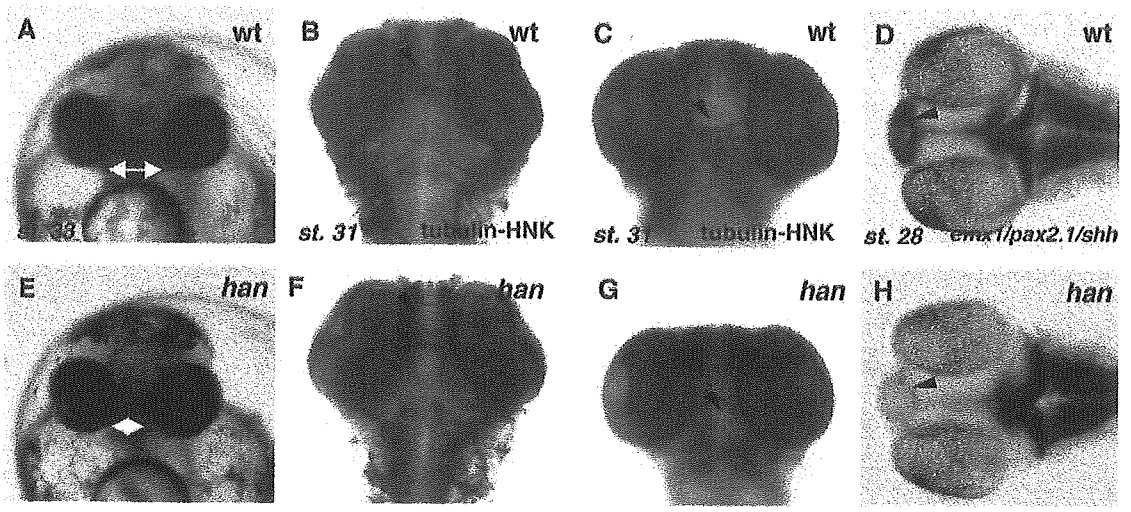

Fig. 4. *han*$^{j41\text{-}3B}$ mutant phenotypes. (A–D) wild type. (E–H) *han* mutant. (A,E) Live phenotype of embryos at st. 33. Anterior front view. Arrows show the width of the telencephalon. (B,C,F,G) Whole-mount staining of embryos at st. 31 with anti-acetylated-tubulin and HNK antibodies. (B,F) Ventral view; (C,G) Anterior front view. Arrowheads show the position of the trigeminal nerve. (D,H) Whole-mount in situ hybridization with *emx1/pax2.1/shh* probe mixture. Dorsal view of embryos at st. 28.

2.4. Class 2 mutations affecting the morphology of the forebrain

Class 2 mutations affecting forebrain shape without altering telencephalon size was divided into the subclasses, 2A to 2C, based on other associated phenotypes (Tables 1 and 2).

2.4.1. Class 2A mutations affecting the forebrain ventricle

We have identified mutations in 6 genes affecting the formation of the forebrain ventricle. In *sarudahiko* (*sar*$^{j106\text{-}4A}$) and *tengu* (*ten*$^{jr10\text{-}4D}$) mutant embryos, the ventricle of the forebrain did not inflate (arrowheads in Fig. 6A–C), the *emx1* expression did not extend ventrally as in the wild type (black arrowheads in Fig. 6P–R), while the *dlx2* expression remained normal (data not shown). It is remarkable that the *shh* expression in either the brain or the floor plate was absent, suggesting a defect in midline signaling (white arrowheads in Fig. 6Q,R). At the histological level, neuroepithelial cells in the forebrain and cortical layers of the retina were round and did not exhibit the characteristic polarized cell morphology (Fig. 6F–H,K–M). The defect at the cellular level may account for the defect in the histogenesis of the forebrain ventricle in these mutants. *sar* and *ten* mutants also shared a common defect in the cardiovascular system.

In *karuna* (*kar*$^{j50\text{-}4A}$) and *oobesshimi* (*oob*$^{j103\text{-}11A}$) mutant embryos, in contrast, the forebrain ventricle was abnormally expanded (arrowheads in Fig. 6A,D–F,I,J). *kar* mutant embryos also had small eyes (Fig. 6D,I), and a forebrain ventricle open on the ventral side (open arrowhead in Fig. 6I). The *shh* expression in the diencephalon was altered in *kar* mutant embryos (white and black arrowheads in Fig. 6S), suggesting that the patterning of the ventral forebrain is affected. In addition, the bilateral retinas were not completely separated in the midline (black arrowhead in Fig. 6I). It is interesting to determine whether this is caused by the altered development of the optic stalk or by a defect in the morphogenetic movement of diencephalon to split

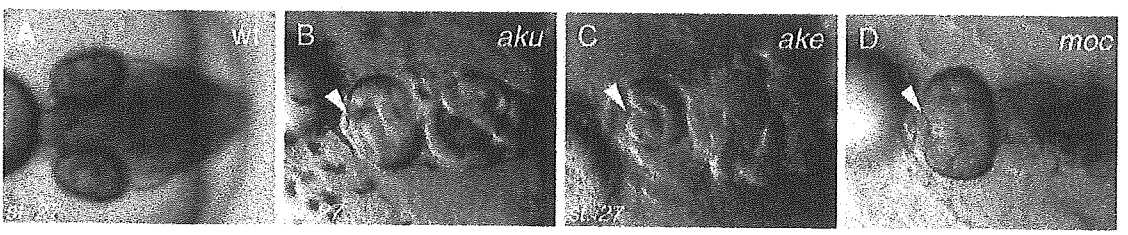

Fig. 5. Mutants in 3 genes display phenotypes similar to that of *oep* zebrafish mutants. (A–D) Dorsal view of st. 27 live embryos of (A) wild-type; (B) *aku*$^{j22\text{-}15A}$ mutant; (C) *ake*$^{j54\text{-}7A}$ mutant and (D) *moc*$^{j96\text{-}11B}$ mutant.

Table 2
Defects in the axonal scaffolds and the gene expressions in the forebrain

Class	Genes	Structures									
		Anti-tubulin + HNK-1				*Emx1*	*Dlx2*		*Shh*		
		AC	SOT	OF	ON	dTel	vTel	vTha	Zli	vFor	Hth
Class 1A	*ket*	def	−	+	+	r	−	as	−	dve	ape
Class 1B	*aon*	def	−	−	+	vs	ps and r	ps and r	−	+	r
	kob	+	+	def	+	ve	ps and r	ps and r	r	r	+
	bou	def	−	def	def	apr	+	f	f	f	f
	nop	nj	nj	−	nj	r	−	as	−	+	pe
Class 2A	*sar*	nd	nd	nd	nd	de and vr	+	+	−	−	−
	ten	+	+	+	r	vr	+	+	−	−	−
	kar	nd	nd	nd	nd	ve	ps	ps and ve	+	+	r
	oob	nd	nd	nd	nd	+	ps and vr	ps and vr	r	r	r

AC, anterior commissure; For, forebrain; Hth, hypothalamus; OF, olfactory nerve; ON, optic nerve; SOT, supraoptic tract; Tel, telencephalon; Tha, thalamus; Zli, zona limitans intrathalamica; +, less affected; −, missing; r, reduced; e, expanded; s, shifted; f, fragmented; def, defasciculated; nj, not judgeable; nd, not done; a, anteriorly; p, posteriorly; d, dorsally; v, ventrally.

a single retinal field into bilateral optic primordia (Varga et al., 1999).

In *oob* mutant embryos, the enlarged ventricle could be observed from st. 25. The roof layer of the telencephalon appeared to be absent and the telencephalon became swollen at later stages (arrowhead in Fig. 6J). Despite the malformation of the forebrain ventricle, the cells in the neuroepithelium were normally polarized (Fig. 6J,O), and

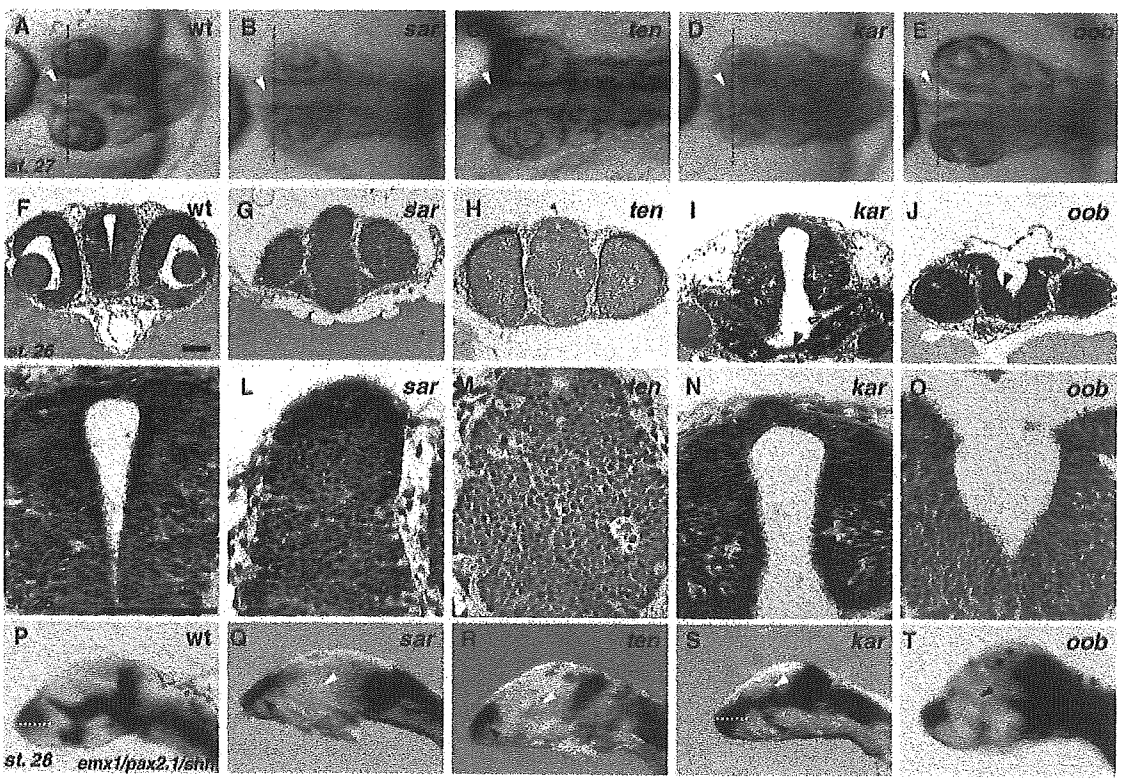

Fig. 6. Class 2A mutant phenotypes. (A,F,K,P) Wild type; (B,G,L,Q) *sar*$^{j106\text{-}4A}$; (C,H,M,R) *ten*$^{jr10\text{-}4D}$; (D,I,N,S) *kar*$^{j50\text{-}4A}$; (E,J,O,T) *oob*$^{j103\text{-}11A}$ embryos. (A–E) Live phenotypes of Class 2A mutant embryos at st. 27 (dorsal view). Arrowheads show the forebrain ventricle. (F–J) Transverse sections of embryos at st. 26, stained with hematoxylin and eosin. (K–O) A higher magnification image of the transverse sections, focused on the cell layers around the forebrain ventricle. (P–T) Whole-mount in situ hybridization analysis of embryos at st. 28 with *emx1/pax2.1/shh* probe mixture. Lateral view of the brain. Scale bar, 50 μm.

the general pattern of gene expression was not significantly affected, except for the reduction in *shh* expression in the diencephalon (arrowhead in Fig. 6T).

2.4.2. Class 2B mutations affecting formation of anterior commissure

Anterior commissure nerves connect the two telencephalic hemispheres. We have identified two genes required for the formation of the commissure of bilateral axons from the dorsal telencephalon (Class 2B mutants).

In *shikami* (*shi*$^{j92\text{-}3A}$) mutant embryos, axons from the bilateral telencephalic halves did not associate with each other at the midline (arrowhead in Fig. 7D). Interestingly, it appears that axons originating from one side of the telencephalon crossed once to the other side then returned to the midline. The telencephalon tended to be distorted in *shi* mutant embryos (arrowhead in Fig. 7C).

In *ikazuchi* (*ika*$^{j94\text{-}8A}$) mutant embryos, axons from telencephalic clusters defasciculated and formed ectopic minor commissures in the dorsal telencephalon (arrowhead in Fig. 7F). The forebrain of *ika* was slightly enlarged (arrowhead in Fig. 7E).

2.4.3. The baltan mutation of Class 2D with a unique set of forebrain defects

baltan (*bal*$^{j102\text{-}2A}$) mutant embryos were recognized by an early focal neural degeneration in the forebrain, leading to a reduction of the forebrain size and an edema (Fig. 8A,G). Surprisingly, staining of axons of cranial nerves revealed that many axons crossed the midline at various A–P levels, causing a ladderlike appearance (arrowheads in Fig. 8B,H). The bilateral optic nerve did not form a chiasm between the eyes but crossed the midline at the anterior commissure (arrowheads in Fig. 8C,I). The *emx1* expression was absent and the *dlx2* expression in the ventral telencephalon was attenuated (black arrowheads in Fig. 8D,E,J,K). *dlx2* expression in the ventral thalamus was markedly reduced (white arrowheads in Fig. 8E,K), suggesting a seriously defective regionalization of the forebrain in the *baltan*

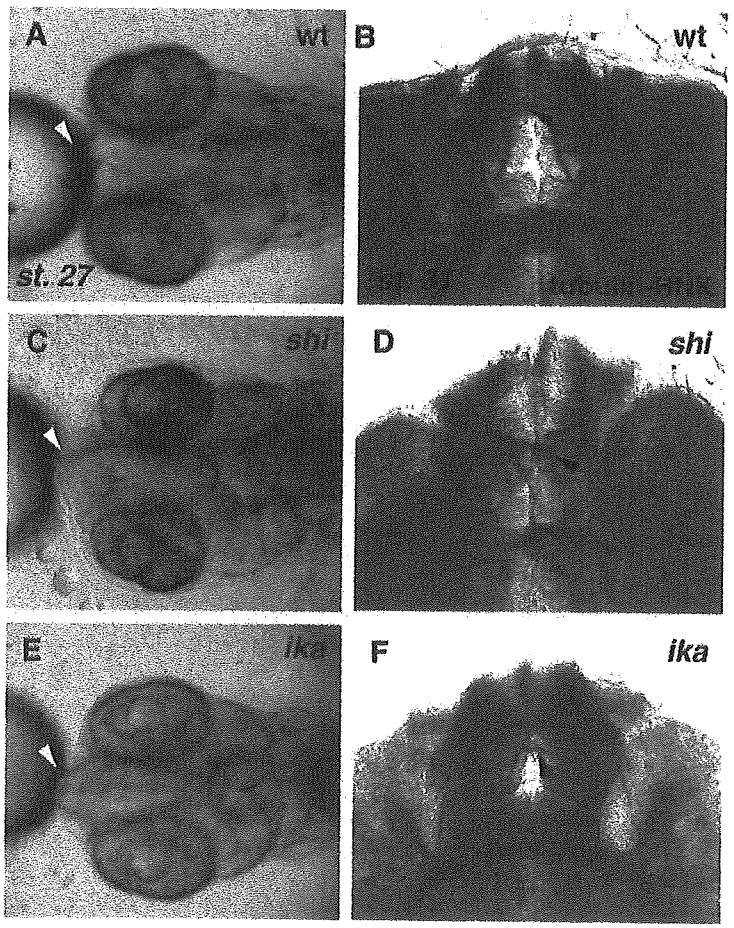

Fig. 7. Class 2B mutant phenotypes. (A,B) wild type; (C,D) *shi*$^{j92\text{-}3A}$; (E,F) *ika*$^{j94\text{-}8A}$. (A,C,E) Morphology of Class 2B mutant embryos at st. 27 (dorsal view). (B,D,F) Whole-mount staining of embryos at st. 31 with anti-acetylated-tubulin and HNK antibodies. Arrowheads show the anterior commissure.

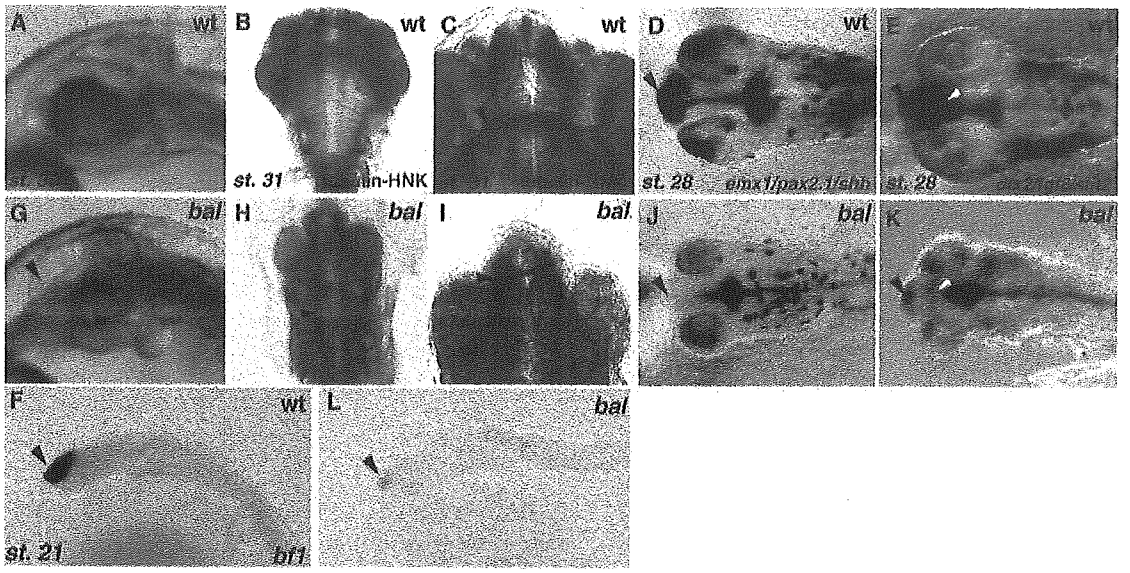

Fig. 8. $bal^{j102\text{-}2A}$ mutant phenotypes. (A–F) Wild type; (G–L) $bal^{j102\text{-}2A}$ embryos. (A,G) Live embryos of wild-type (A) and (G) $bal^{j102\text{-}2A}$ mutant at st. 30 (lateral view). An arrowhead in G shows an empty space generated by degeneration in the forebrain. (B,C,H,I) Whole-mount immunostaining of st. 31 embryos using anti-acetylated tubulin and HNK antibodies. (B,H) Ventral view of the head. An arrowhead indicates ladder like axons of unknown origin. (C,I) enlarged view of (B,H). an arrowhead shows the optic nerve. (D–F,J–L) Whole-mount in situ hybridization analysis of embryos at st.28 (D,E,J,K, dorsal view) and st.21 (F,L, lateral view), using (D,J) *emx1/pax2.1/shh*; (E,K) *dlx2/fgf8/slit2* and (F,L) *bf1* as probes. (F,L) Arrowheads indicate the *bf1* expression in the telencephalon.

mutant. Moreover, *bf1* expression at the induction phase of telencephalon was remarkably reduced (Fig. 8F,L). These results suggested that *bal* is necessary for early specification of the forebrain as well as proper axonal projection of cranial nerves.

3. Discussion

3.1. Class 1 mutations causing smaller telencephalon

ket mutants are remarkable for their compromised expression of the early telencephalon marker *bf1*(Fig. 3). In parallel, both *emx1* expression in the dorsal telencephalon and the *dlx2* expression in the ventral telencephalon are strongly reduced, raising the possibility that *ket* is a key regulator required for specification of the telencephalon (Fig. 2N,T). The phenotype of *ket* mutants is reminiscent of that of the *bf1* knockout mouse with hypoplasia of the cerebral hemispheres and more severe defects in the basal region of the telencephalon (Dou et al., 1999). The expression of both *bf1* and *emx1* is reduced in *tlc*- knockdown embryos after the injection of antisense morpholino oligonucleotides (Houart et al., 2002). The possible genetic linkage of *ket* with *bf1* and *tlc* is currently under investigation. In mice, Fgf8 induces *bf1* expression under in vitro culture condition of the forebrain tissue (Shimamura and Rubenstein, 1997). However, telencephalon is somehow formed in the *fgf8* mutants of mice and zebrafish, suggesting it alone is not responsible for induction of the telencephalon (Meyers et al., 1998; Reifers et al., 1998; Shanmugalingam et al., 2000; Shinya et al., 2001).

The major feature of *aon* and *kob* mutants is their defect in dorsoventral (D–V) patterning in the telencephalon. The tissue area for *emx1* expression in the dorsal telencephalon expands or shifts ventrally, and the *dlx2* expression in the ventral telencephalon is reduced and posteriorly displaced (Fig. 2O,P,U,V).

shh-null mice lack any signs of the medial ganglionic eminence (MGE), which is the ventral portion of the basal ganglia, indicating that Shh is required for the patterning of the ventral telencephalon (Chiang et al., 1996). However, it is yet to be determined which part of *shh* expression in the forebrain is required for the D–V patterning of the telencephalon. All the Class 1 mutants have an altered *shh* expression, particularly in the zli (Fig. 2N–R). The zli not only forms a clear histological border between the dorsal and ventral thalami (Larsen et al., 2001), but, for its *shh* expression, is considered to function as a secondary organizing center. The presence of patterning defects of the telencephalon in Class 2 mutants corroborates this notion.

It is to be noted that the phenotype of the Class 1 mutants associated with the decreased expression of *shh* in the forebrain does not resemble those of zebrafish mutants defective in sonic hedgehog signaling, *sonic you* (*syu*),

detour (*dtr*), *you-too* (*yot*) and *slow-muscle-omitted* (*smu*), in which *shh, gli1, gli2, foxh1* and *smoothened*, respectively, are mutated and the primary causes are defects in the midline tissues (Schauerte et al., 1998; Karlstrom et al., 1999; Barresi et al., 2000; Chen et al., 2001; Varga et al., 2001; Karlstrom et al., 2003).

The phenotype of the *nop* mutant, characterized by the expansion of the diencephalon and mesencephalon at the expense of the telencephalon tissue (Fig. 2F), is reminiscent of those of *masterblind(mbl)* and *headless* (*hdl*) mutants of zebrafish. In these zebrafish mutants, the genes coding for the negative regulators of Wnt signaling, *tcf3* and *axin1*, respectively, are mutated, possibly resulting in the over-activation of Wnt signaling throughout the forebrain (Kim et al., 2000; Heisenberg et al., 2001). It is also known that a secreted Wnt antagonist *tlc* is expressed in the anterior neural ridge (Houart et al., 2002). Whether the *nop* gene function is involved in Wnt signaling is of an immediate interest.

3.2. Patterning defects resulting in defective formation of forebrain ventricle

sar and *ten* mutants lack polarized cell shape in the neuroepithelium on one hand (Fig. 6L,M), and show an attenuated *shh* expression in the forebrain and spinal cord on the other (Fig. 6Q,R). It is currently under investigation how these phenotypes correlate with each other.

In *oob* mutants showing the expansion of the forebrain ventricle, the roof plate is missing and the basal plate is thicker (Fig. 6J). This phenotype may reflect an altered D–V patterning or a defect in the histogenetic process dependent on cell–cell interactions. It is interesting to note that the phenotype of *oob* mutants somewhat resembles that of the zebrafish *parachute* mutant of the N-cadherin gene (Lele et al., 2002; Erdmann et al., 2003).

3.3. Mutations affecting axonal paths in the forebrain

Class 2B mutants have characteristic defects in the formation of the anterior commissure. Interestingly, the formation of the anterior commissure is affected differently in *shi* and *ika* mutants, suggesting that *shi* and *ika* may be required for a distinct process in anterior commissure formation (Fig. 7).

It is suggested in zebrafish that a commissure is formed through three steps (Bak and Fraser, 2003). The first step is the extension of the leader axon toward the midline through the already defined axonal tract. The growth cone senses and integrates attractive and repulsive midline cues for their behavior. The second step is the growth and extension of the follower axon along the leader axon toward the midline and its fasciculation with the leader axon. The third step is the interaction of the axons with the leader axon of the opposite side across the midline and mutual fasciculation. In this way, the leader axons from two sides cooperate with each other to establish a commisure across the midline.

In *ika* mutants, the first step may be disturbed since the anterior commisure was formed but in an ectopic position (Fig. 7F). The group of Class 1 mutants, *bou, ket* and *aon*, may have a defect in the second step. The failure of the axons to properly cross the midline in *bou* mutants may be explained by the loss of interaction between the leader and follower axons (Fig. 2K). In *ket* and *aon* mutants, a mild defasciculation of axons in the anterior commissure was observed (Fig. 2H,I).

In *bal* mutants, the anterior commissure and optic nerve joined together. In the region between the anterior commissure and the optic nerve, Netrins, the repulsive cues for axons, are known to be expressed. Indeed, the *netrin* expression in this region was altered in *noi* and *ace* zebrafish mutant embryos, accompanied by abnormalities of the anterior and postoptic commissures (Macdonald et al., 1997; Shanmugalingam et al., 2000). It would be interesting to determine whether the *netrin* expression between the anterior commissure and the optic nerve is altered in *bal* mutants. In *shi* mutants, the third step may be affected, since the commissure structure crossing the midline was not established.

In the Class 1 mutants which have altered gene expression pattern, the formation of axonal scaffolds in the forebrain is also affected, as summarized in Table 2. In zebrafish, the boundaries of regulatory gene expression domains correspond in many cases to early axonal scaffolds in the forebrain (Macdonald et al., 1994). It has been hypothesized that a growth cone extends along the interface between two domains of cells with different cell surface properties. Class 1 Medaka mutants should prove useful in testing this hypothesis.

3.4. Medaka and zebrafish complement to genetically dissect forebrain formation

We have identified 25 loci required for the formation of the forebrain in the systematic screen in Medaka. Although screenings covering the whole genome have already been carried out in zebrafish, we identified a battery of mutations resulting in phenotypes that were not observed in the zebrafish mutant collection. This could reflect (1) the difference in the functional overlap of genes, (2) the difference in the regulation of forebrain development, (3) the difference in susceptibility to mutagens of a genetic locus between Medaka and zebrafish.

Some other mutant phenotypes corresponded to those of identified zebrafish mutants. These mutated genes of shared phenotypes must be involved in the genetic pathways conserved between the two species. Interestingly, mutations in 3 genes, *aku, ake* and *moc* of Class 1D result in a phenotype similar to that of *one-eyed-pinhead* (*oep*) in zebrafish (Schier et al., 1997; Strahle et al., 1997). In zebrafish, mutants of other genes involved in Nodal

signaling, *cyclops*(*cyc*), *squint* (*sqt*), and *schmalspur* (*sur*) displayed slightly different phenotypes, suggesting a divergence of the molecular components in a signaling pathway between the two species (Hatta et al., 1994; Brand et al., 1996b; Malicki et al., 1996; Schier et al., 1996; Heisenberg and Nusslein-Volhard, 1997; Feldman et al., 1998; Rebagliati et al., 1998; Sampath et al., 1998; Pogoda et al., 2000; Sirotkin et al., 2000). Similarly, mutations in 3 genes, *oob, sam,* and *sgu,* caused phenotypes that are reminiscent of those of *parachute* zebrafish mutant of the N-cadherin gene. No mutations in other genes are reported in zebrafish to cause the *parachute* phenotype (Lele et al., 2002; Erdmann et al., 2003). Cloning of these mutated genes in Medaka and the analysis of their function will reveal both conserved and divergent functions of the genes essential for forebrain formation. The results of the mutant screen in Medaka do demonstrate that zebrafish and Medaka complement each other in uncovering more genes and more functions involved in the developmental process.

4. Experimental procedures

4.1. Mutant embryos

Fish are mutagenized and screened for mutations as described in an accompanying paper (Furutani-Seiki et al., this issue). Mutant embryos were obtained by mating heterozygotes, reared at 28 °C, and staged according to the development of sibling normal embryos. Live embryos were photographed after removing the chorion and mounting in 2.5% methylcellulose.

4.2. Histological methods

Whole-mount staining of the embryos by in situ hybridization or with anti-acetylated tubulin/anti-HNK1 antibodies was performed as described by Hammerschmidt and Nusslein-Volhard (1993). RNA probes for in situ hybridization were labeled with digoxygenin, and detected using an anti-digoxygenin antibody conjugated with alkalinephophatase, and reacted with BM purple (Roche) for color development. For histological sections, the embryos were fixed in 4% paraformaldehyde, dehydrated through ethanol series and embedded in Jung HistoResin Plus (Leica) and sections 4 μm thickness of were made.

Acknowledgements

We are grateful to Dr Giselbert Hauptmann for input about regionalization of medaka brain, Drs Takashi Sasaki and Noboru Nakajima for cloning *slit2, dlx2* and *bf1* probes. This work was supported by the ERATO project of the Japan Science and Technology Agency to H.K.

References

Bak, M., Fraser, S.E., 2003. Axon fasciculation and differences in midline kinetics between pioneer and follower axons within commissural fascicles. Development 130, 4999–5008.

Barresi, M.J., Stickney, H.L., Devoto, S.H., 2000. The zebrafish slow-muscle-omitted gene product is required for Hedgehog signal transduction and the development of slow muscle identity. Development 127, 2189–2199.

Brand, M., Heisenberg, C.P., Jiang, Y.J., Beuchle, D., Lun, K., Furutani-Seiki, M., et al., 1996a. Mutations in zebrafish genes affecting the formation of the boundary between midbrain and hindbrain. Development 123, 179–190.

Brand, M., Heisenberg, C.P., Warga, R.M., Pelegri, F., Karlstrom, R.O., Beuchle, D., et al., 1996b. Mutations affecting development of the midline and general body shape during zebrafish embryogenesis. Development 123, 129–142.

Bulfone, A., Puelles, L., Porteus, M.H., Frohman, M.A., Martin, G.R., Rubenstein, J.L., 1993. Spatially restricted expression of Dlx-1, Dlx-2 (Tes-1), Gbx-2, and Wnt-3 in the embryonic day 12.5 mouse forebrain defines potential transverse and longitudinal segmental boundaries. J. Neurosci. 13, 3155–3172.

Chen, W., Burgess, S., Hopkins, N., 2001. Analysis of the zebrafish smoothened mutant reveals conserved and divergent functions of hedgehog activity. Development 128, 2385–2396.

Chiang, C., Litingtung, Y., Lee, E., Young, K.E., Corden, J.L., Westphal, H., Beachy, P.A., 1996. Cyclopia and defective axial patterning in mice lacking Sonic hedgehog gene function. Nature 383, 407–413.

Dou, C.L., Li, S., Lai, E., 1999. Dual role of brain factor-1 in regulating growth and patterning of the cerebral hemispheres. Cereb. Cortex 9, 543–550.

Erdmann, B., Kirsch, F.P., Rathjen, F.G., More, M.I., 2003. N-cadherin is essential for retinal lamination in the zebrafish. Dev. Dyn. 226, 570–577.

Feldman, B., Gates, M.A., Egan, E.S., Dougan, S.T., Rennebeck, G., Sirotkin, H.I., et al., 1998. Zebrafish organizer development and germ-layer formation require nodal-related signals. Nature 395, 181–185.

Fernandez, A.S., Pieau, C., Reperant, J., Boncinelli, E., Wassef, M., 1998. Expression of the Emx-1 and Dlx-1 homeobox genes define three molecularly distinct domains in the telencephalon of mouse, chick, turtle and frog embryos: implications for the evolution of telencephalic subdivisions in amniotes. Development 125, 2099–2111.

Figdor, M.C., Stern, C.D., 1993. Segmental organization of embryonic diencephalon. Nature 363, 630–634.

Furutani-Seiki, M., Jiang, Y.J., Brand, M., Heisenberg, C.P., Houart, C., Beuchle, D., et al., 1996. Neural degeneration mutants in the zebrafish, *Danio rerio*. Development 123, 229–239.

Hatta, K., Puschel, A.W., Kimmel, C.B., 1994. Midline signaling in the primordium of the zebrafish anterior central nervous system. Proc. Natl Acad. Sci. USA 91, 2061–2065.

Hauptmann, G., Gerster, T., 2000. Regulatory gene expression patterns reveal transverse and longitudinal subdivisions of the embryonic zebrafish forebrain. Mech. Dev. 91, 105–118.

Hauptmann, G., Soll, I., Gerster, T., 2002. The early embryonic zebrafish forebrain is subdivided into molecularly distinct transverse and longitudinal domains. Brain Res. Bull. 57, 371–375.

Heisenberg, C.P., Nusslein-Volhard, C., 1997. The function of silberblick in the positioning of the eye anlage in the zebrafish embryo. Dev. Biol. 184, 85–94.

Heisenberg, C.P., Brand, M., Jiang, Y.J., Warga, R.M., Beuchle, D., van Eeden, F.J., et al., 1996. Genes involved in forebrain development in the zebrafish, *Danio rerio*. Development 123, 191–203.

Heisenberg, C.P., Houart, C., Take-Uchi, M., Rauch, G.J., Young, N., Coutinho, P., et al., 2001. A mutation in the Gsk3-binding domain of zebrafish Masterblind/Axin1 leads to a fate transformation of telencephalon and eyes to diencephalon. Genes Dev. 15, 1427–1434.

Houart, C., Westerfield, M., Wilson, S.W., 1998. A small population of anterior cells patterns the forebrain during zebrafish gastrulation. Nature 391, 788–792.

Houart, C., Caneparo, L., Heisenberg, C., Barth, K., Take-Uchi, M., Wilson, S., 2002. Establishment of the telencephalon during gastrulation by local antagonism of Wnt signaling. Neuron 35, 255–265.

Ishikawa, Y., Hyodo-Taguchi, Y., 1994. Cranial nerves and brain fiber systems of the medaka fry as observed by a whole-mount staining method. Neurosci. Res. 19, 379–386.

Iwamatsu, T., 1994. Stages of normal development in the medaka *Oryzias latipes*. Zool. Sci. 11, 825–839.

Karlstrom, R.O., Talbot, W.S., Schier, A.F., 1999. Comparative synteny cloning of zebrafish you-too: mutations in the Hedgehog target gli2 affect ventral forebrain patterning. Genes Dev. 13, 388–393.

Karlstrom, R.O., Tyurina, O.V., Kawakami, A., Nishioka, N., Talbot, W.S., Sasaki, H., Schier, A.F., 2003. Genetic analysis of zebrafish gli1 and gli2 reveals divergent requirements for gli genes in vertebrate development. Development 130, 1549–1564.

Kim, C.H., Oda, T., Itoh, M., Jiang, D., Artinger, K.B., Chandrasekharappa, S.C., et al., 2000. Repressor activity of Headless/Tcf3 is essential for vertebrate head formation. Nature 407, 913–916.

Larsen, C.W., Zeltser, L.M., Lumsden, A., 2001. Boundary formation and compartition in the avian diencephalon. J. Neurosci. 21, 4699–4711.

Lele, Z., Folchert, A., Concha, M., Rauch, G.J., Geisler, R., Rosa, F., et al., 2002. parachute/n-cadherin is required for morphogenesis and maintained integrity of the zebrafish neural tube. Development 129, 3281–3294.

Macdonald, R., Xu, Q., Barth, K.A., Mikkola, I., Holder, N., Fjose, A., et al., 1994. Regulatory gene expression boundaries demarcate sites of neuronal differentiation in the embryonic zebrafish forebrain. Neuron 13, 1039–1053.

Macdonald, R., Scholes, J., Strahle, U., Brennan, C., Holder, N., Brand, M., Wilson, S.W., 1997. The Pax protein Noi is required for commissural axon pathway formation in the rostral forebrain. Development 124, 2397–2408.

Malicki, J., Neuhauss, S.C., Schier, A.F., Solnica-Krezel, L., Stemple, D.L., Stainier, D.Y., et al., 1996. Mutations affecting development of the zebrafish retina. Development 123, 263–273.

Mathieu, J., Barth, A., Rosa, F.M., Wilson, S.W., Peyrieras, N., 2002. Distinct and cooperative roles for Nodal and Hedgehog signals during hypothalamic development. Development 129, 3055–3065.

Meyers, E.N., Lewandoski, M., Martin, G.R., 1998. An Fgf8 mutant allelic series generated by Cre- and Flp-mediated recombination. Nat. Genet. 18, 136–141.

Pogoda, H.M., Solnica-Krezel, L., Driever, W., Meyer, D., 2000. The zebrafish forkhead transcription factor FoxH1/Fast1 is a modulator of nodal signaling required for organizer formation. Curr. Biol. 10, 1041–1049.

Puelles, L., Rubenstein, J.L., 1993. Expression patterns of homeobox and other putative regulatory genes in the embryonic mouse forebrain suggest a neuromeric organization. Trends Neurosci. 16, 472–479.

Puelles, L., Kuwana, E., Puelles, E., Bulfone, A., Shimamura, K., Keleher, J., et al., 2000. Pallial and subpallial derivatives in the embryonic chick and mouse telencephalon, traced by the expression of the genes Dlx-2, Emx-1, Nkx-2.1, Pax-6, and Tbr-1. J. Comp. Neurol. 424, 409–438.

Rallu, M., Corbin, J.G., Fishell, G., 2002. Parsing the prosencephalon. Nat. Rev. Neurosci. 3, 943–951.

Rebagliati, M.R., Toyama, R., Haffter, P., Dawid, I.B., 1998. Cyclops encodes a nodal-related factor involved in midline signaling. Proc. Natl Acad. Sci. USA 95, 9932–9937.

Reifers, F., Bohli, H., Walsh, E.C., Crossley, P.H., Stainier, D.Y., Brand, M., 1998. Fgf8 is mutated in zebrafish acerebellar (ace) mutants and is required for maintenance of midbrain–hindbrain boundary development and somitogenesis. Development 125, 2381–2395.

Rohr, K.B., Barth, K.A., Varga, Z.M., Wilson, S.W., 2001. The nodal pathway acts upstream of hedgehog signaling to specify ventral telencephalic identity. Neuron 29, 341–351.

Sampath, K., Rubinstein, A.L., Cheng, A.M., Liang, J.O., Fekany, K., Solnica-Krezel, L., et al., 1998. Induction of the zebrafish ventral brain and floorplate requires cyclops/nodal signalling. Nature 395, 185–189.

Schauerte, H.E., van Eeden, F.J., Fricke, C., Odenthal, J., Strahle, U., Haffter, P., 1998. Sonic hedgehog is not required for the induction of medial floor plate cells in the zebrafish. Development 125, 2983–2993.

Schier, A.F., Neuhauss, S.C., Harvey, M., Malicki, J., Solnica-Krezel, L., Stainier, D.Y., et al., 1996. Mutations affecting the development of the embryonic zebrafish brain. Development 123, 165–178.

Schier, A.F., Neuhauss, S.C., Helde, K.A., Talbot, W.S., Driever, W., 1997. The one-eyed pinhead gene functions in mesoderm and endoderm formation in zebrafish and interacts with no tail. Development 124, 327–342.

Shanmugalingam, S., Houart, C., Picker, A., Reifers, F., Macdonald, R., Barth, A., et al., 2000. Ace/Fgf8 is required for forebrain commissure formation and patterning of the telencephalon. Development 127, 2549–2561.

Shimamura, K., Rubenstein, J.L., 1997. Inductive interactions direct early regionalization of the mouse forebrain. Development 124, 2709–2718.

Shinya, M., Koshida, S., Sawada, A., Kuroiwa, A., Takeda, H., 2001. Fgf signalling through MAPK cascade is required for development of the subpallial telencephalon in zebrafish embryos. Development 128, 4153–4164.

Sirotkin, H.I., Gates, M.A., Kelly, P.D., Schier, A.F., Talbot, W.S., 2000. Fast1 is required for the development of dorsal axial structures in zebrafish. Curr. Biol. 10, 1051–1054.

Strahle, U., Jesuthasan, S., Blader, P., Garcia-Villalba, P., Hatta, K., Ingham, P.W., 1997. One-eyed pinhead is required for development of the ventral midline of the zebrafish (*Danio rerio*) neural tube. Genes Funct. 1, 131–148.

Tao, W., Lai, E., 1992. Telencephalon-restricted expression of BF-1, a new member of the HNF-3/fork head gene family, in the developing rat brain. Neuron 8, 957–966.

Varga, Z.M., Wegner, J., Westerfield, M., 1999. Anterior movement of ventral diencephalic precursors separates the primordial eye field in the neural plate and requires cyclops. Development 126, 5533–5546.

Varga, Z.M., Amores, A., Lewis, K.E., Yan, Y.L., Postlethwait, J.H., Eisen, J.S., Westerfield, M., 2001. Zebrafish smoothened functions in ventral neural tube specification and axon tract formation. Development 128, 3497–3509.

Wilson, S.W., Rubenstein, J.L., 2000. Induction and dorsoventral patterning of the telencephalon. Neuron 28, 641–651.

ELSEVIER

Mechanisms of Development 121 (2004) 791–802

www.elsevier.com/locate/modo

Research paper

Mutations affecting liver development and function in Medaka, *Oryzias latipes*, screened by multiple criteria

Tomomi Watanabe[a], Satoshi Asaka[a], Daiju Kitagawa[a], Kota Saito[a], Ryumei Kurashige[a], Takao Sasado[b], Chikako Morinaga[b], Hiroshi Suwa[b], Katsutoshi Niwa[b], Thorsten Henrich[b], Yukihiro Hirose[c], Akihito Yasuoka[d], Hiroki Yoda[e], Tomonori Deguchi[e], Norimasa Iwanami[f], Sanae Kunimatsu[f], Masakazu Osakada[e], Felix Loosli[h], Rebecca Quiring[h], Matthias Carl[h], Clemens Grabher[h], Sylke Winkler[h], Filippo Del Bene[h], Joachim Wittbrodt[h], Keiko Abe[d], Yousuke Takahama[f], Katsuhito Takahashi[g], Toshiaki Katada[a], Hiroshi Nishina[a,*], Hisato Kondoh[b], Makoto Furutani-Seiki[b,*]

[a]*Department of Physiological Chemistry, Graduate School of Pharmaceutical Sciences, University of Tokyo, Tokyo 113-0033, Japan*
[b]*ERATO, Jaman Science and Technology Corporation, Kondoh Differentiation Signaling Project, Kawara-cho 14, Yoshida, Sakyo-ku, Kyoto 606-8305, Japan*
[c]*Graduate School of Biostudies, Kyoto University, Kyoto 606-8501, Japan*
[d]*Department of Applied Biological Chemistry, University of Tokyo, Tokyo 113-0033, Japan*
[e]*Graduate School of Frontier Biosciences, Osaka University, Osaka 565-0871, Japan*
[f]*Division of Experimental Immunology, Institute for Genome Research, The University of Tokushima, Tokushima 770-8503, Japan*
[g]*Department of Molecular Medicine and Pathophysiology, Research Institute, Osaka Medical Center for Cancer and Cardiovascular Diseases, Osaka 537-8511, Japan*
[h]*Developmental Biology Programme, EMBL Heidelberg, Meyerhofstrasse 1, D-69117, Heidelberg, Germany*

Received 20 January 2004; received in revised form 30 March 2004; accepted 3 April 2004

Abstract

We report here mutations affecting various aspects of liver development and function identified by multiple assays in a systematic mutagenesis screen in Medaka. The 22 identified recessive mutations assigned to 19 complementation groups fell into five phenotypic groups. Group 1, showing defective liver morphogenesis, comprises mutations in four genes, which may be involved in the regulation of growth or patterning of the gut endoderm. Group 2 comprises mutations in three genes that affect the laterality of the liver; in *kendama* mutants of this group, the laterality of the heart and liver is uncoupled and randomized. Group 3 includes mutations in three genes altering bile color, indicative of defects in hemoglobin–bilirubin metabolism and *globin* synthesis. Group 4 consists of mutations in three genes, characterized by a decrease in the accumulation of fluorescent metabolite of a phospholipase A_2 substrate, PED6, in the gall bladder. Lipid metabolism or the transport of lipid metabolites may be affected by these mutations. Mutations in Groups 3 and 4 may provide animal models for relevant human diseases. Group 5 mutations in six genes affect the formation of endoderm, endodermal rods and hepatic bud from which the liver develops. These Medaka mutations, identified by morphological and metabolite marker screens, should provide clues to understanding molecular mechanisms underlying formation of a functional liver.

Keywords: Liver development; Medaka; Hepatoblast; Hepatic bud; Laterality; Gall bladder; Lipid metabolism; Endoderm formation; Bile; Zebrafish

1. Introduction

The liver is an organ with vital functions, including processing and storage of nutrients, maintenance of serum composition, detoxification and bile production. The major functional cells of a liver are the hepatocytes

* Corresponding authors. Tel.: +81-75-771-9362; fax: +81-75-771-3835 (M. Furutani-Seiki); Tel.: +81-3-5841-4754; fax: +81-3-5841-4751 (H. Nishina).
E-mail addresses: furutani@dsp.jst.go.jp (M. Furutani-Seiki), nishina@mol.f.u-tokyo.ac.jp (H. Nishina).

0925-4773/$ - see front matter © 2004 Elsevier Ireland Ltd. All rights reserved.
doi:10.1016/j.mod.2004.04.004

and cholangiocytes (bile duct cells). The common progenitors of hepatocytes and cholangiocytes are derived from hepatoblasts in the hepatic endoderm. The hepatic endoderm arises from the foregut endoderm that interacts with adjacent tissues, such as the cardiac mesoderm and septum transversum mesenchyme (Douarin, 1975; Grapin-Botton and Melton, 2000; Tam et al., 2003; Zaret, 2001). The vasculature is another important component of the liver. Angioblasts, which are endothelial cell precursors, accumulate around the liver bud and become interspersed with the hepatoblasts (Matsumoto et al., 2001).

Regulatory genes that are crucial for liver formation have been isolated in mice and confirmed by reverse genetics (see Zaret, 2002 for a review). For instance, we have shown using SEK1 or MKK7-deficient mice that two stress-signaling kinases, SEK1 (also called MKK4) and MKK7, play crucial roles in hepatoblast proliferation and survival (Nishina et al., 1999; Wada et al., 2004; Watanabe et al., 2002). Although a reverse genetic approach is powerful in characterizing functions of known genes, knowledge of genes, particularly in hepatic bud formation from endoderm, morphogenesis and laterality of the liver, and hemoglobin–bilirubin or lipid metabolism, is still limited. Therefore, identifying mutations affecting these aspects of liver formation and function will uncover genes required for these processes.

Systematic forward genetic screens for mutations affecting embryogenesis have been carried out in zebrafish. Zebrafish embryos are transparent and sustain defects in circulation or hematopoiesis, because oxygen supplied by simple diffusion is sufficient for development and the liver is not the site of embryonic hematopoiesis (Alexander and Stainier, 1999). These characteristics of zebrafish have enabled the study of genes involved in the development of endoderm, cardiovascular and hematopoietic systems. Zebrafish mutants with impaired endoderm formation, degenerative liver, impaired lipid metabolism in the intestine and hepatobiliary system, have been identified (Chen et al., 1996; Farber et al., 2001; Pack et al., 1996; Schier et al., 1996, 1997; Zhang et al., 1998). Furthermore, the availability of transgenic lines expressing GFP throughout the digestive system allows direct observation of the endoderm and digestive organ formation in living embryos (Field et al., 2003; Ober et al., 2003). However, genes identifiable in a single model organism by the mutational approach are limited due to a functional overlap of genes in vertebrates.

Medaka is evolutionally distant from zebrafish and interspecies differences in the functional overlap of genes allow identification of mutations as yet unidentified in zebrafish. The liver and gall bladder are more conspicuous in living embryos in Medaka than in zebrafish. Medaka has a smaller genome size (half that of zebrafish, and only double that of Fugu), inbred strains are available, and a wide range of growth temperatures facilitates identification of temperature sensitive mutations.

Taking advantage of these attributes of Medaka, we have carried out a mutagenesis screen, using multiple assays to detect defects in various aspects of the development of a functional liver. These include not only morphological assays, but also those of the functions related to the liver, such as hemoglobin–bile and lipid metabolism. In this report, we present the initial characterization of mutations isolated in the screen, ranging from those affecting endoderm formation to those affecting liver physiology in Medaka.

2. Results

2.1. Designing of mutant screening based on multiple criteria

2.1.1. Morphological screening

We carried out the morphological screen of the liver by inspecting live embryos when the liver became discernible from 4 days post-fertilization (dpf, stage (st.) 32) at 28 °C and the gall bladder became prominent at approximately 120 h post-fertilization (hpf, st. 36). The lateral views of wild-type embryos and livers at st. 32 and 36 are shown in Fig. 1A–C. The liver, gall bladder, and blood vessel from the liver connected to the Cuvierian duct developing on the left side of the embryo were observed (Fig. 1B,C).

To analyze the time course of liver development, we carried out in situ hybridization between st. 21 and 39 using endoderm-specific markers, *foxA3* and *gata6* (Fig. 1D–P). The hepatic bud formed from the endoderm rod in wild-type Medaka at st. 25 (Fig. 1H,I). At st. 27 the liver began to enlarge and the swim bladder appeared from the gut tube and began to enlarge (Fig. 1J–P, arrowheads and asterisks indicate the liver and swim bladder, respectively). *foxA3* was also expressed in the pharynx, but unlike in zebrafish, *foxA3* was not expressed in the pancreas in Medaka (data not shown). On the other hand, the expression of *gata6* was restricted to the liver from st. 25 to 31 (Fig. 1I,K,M). Soon after at st. 31, we screened live embryos. No expression of *gata6* was detected in the liver at st. 34 (Fig. 1O). In zebrafish, *gata6* is expressed in the liver and gut. Thus, the expression pattern of *gata6* in Medaka is different from that in zebrafish.

Considering the relatively late development of the liver in embryogenesis, care was taken to avoid isolating mutants showing a general retardation of development. Mutants with altered liver morphologies, such as the size, shape, and laterality of livers, were screened first at st. 32 and confirmed at st. 36 when the liver and gall bladder became larger in wild-type embryos.

2.1.2. Screening of gall bladder color

Based on the assumption that impaired bile metabolism in the liver results in an abnormal color of bile, we inspected

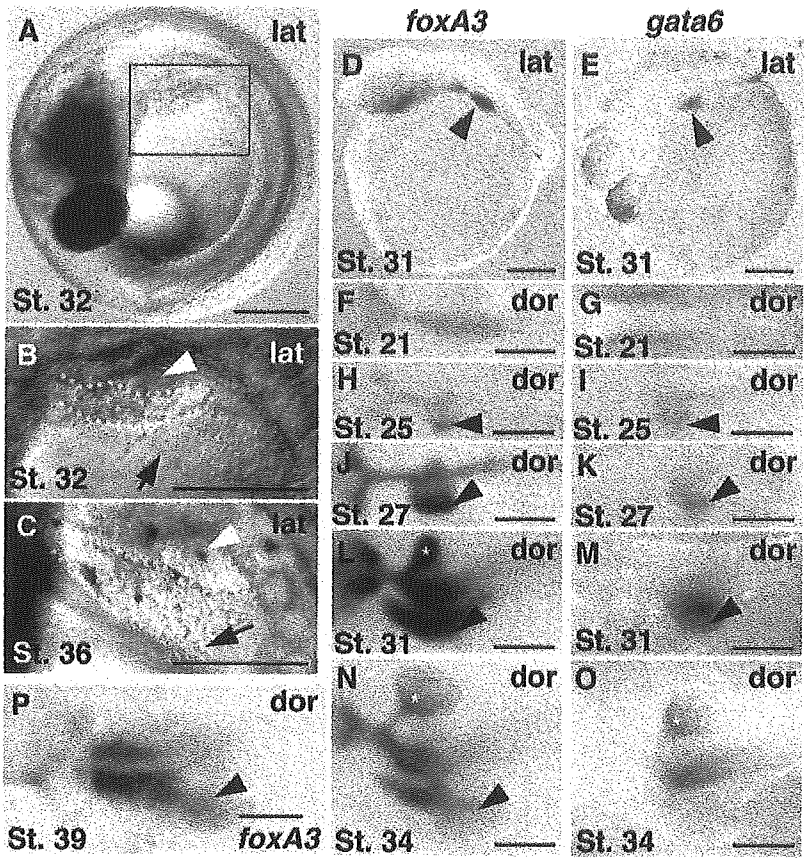

Fig. 1. Liver development in Medaka. Live (A–C) and fixed wild-type embryos stained by in situ hybridization using the *foxA3* (D, F, H, J, L, N, and P) and *gata6* (E, G, I, K, M, and O) probes. (A–C, D, and E) Lateral view; (F–P) Dorsal view. (A–C) The liver was readily visible from the left side of living embryos at st. 32 (A and B) and st. 36 (C) when screening was carried out; (F and G) st. 21; (H and I) The hepatic bud was formed at st. 25 and subsequently liver growth occurred; (J and K) st. 27; (L and M) st. 31; (N and O) st. 34 and (P) st. 39. White broken line demarcates the liver. White arrowheads and black arrows indicate the gall bladder and the vein of the liver, respectively. Black arrowheads and white asterisks show the hepatic bud and the liver, and the swim bladders, respectively. lat: lateral, dor: dorsal. Scale bars correspond to 200 μm.

color of bile in the gall bladder. Bile in the wild-type embryo at st. 35 was light green. Impaired erythropoiesis was reported to alter bile color in zebrafish (Shafizadeh et al., 2002). To distinguish mutations affecting erythropoiesis from those affecting bile metabolism in the liver, we carried out hemoglobin staining with *o*-dianisidine and in situ hybridization analysis using embryonic globins such as *α-0*, *α-1*, and *β-1 globins*.

2.1.3. Screening using fluorescent phospholipid reporters

We used a fluorescent phospholipid reporter, PED6, to screen for mutations affecting lipid metabolism (Farber et al., 2001).

PED6 is a synthetic substrate for PLA_2 that becomes fluorescent after cleavage in the intestine and its fluorescent PED6 metabolites undergo rapid hepatobiliary transport, labeling the liver before the gall bladder, as shown in Fig. 5C. Embryos administered with PED6 showed intense fluorescence in the gall bladder, liver and intestinal lumen. We screened for embryos showing an impaired accumulation of the fluorescent metabolites of PED6. To exclude mutations affecting the swallowing of PED6, the unquenched form of PED6, BODIPY-FL-C5, was used.

2.1.4. Rescreening for mutations affecting early embryogenesis using the foxA3 probe

In addition to directly screening for liver associated phenotypes, we also screened for mutations affecting endoderm and hepatic bud formations among mutants that were initially identified on the basis of morphological abnormalities (Furutani-Seiki et al., 2004). To this end, we carried out in situ hybridization using *foxA3* at st. 28 (Fig. 1J).

2.2. Mutations affecting formation and function of the liver isolated by the multi-assay screen

By screening 210 F2 families, we have isolated 19 mutations. Since all of the mutations were zygotic recessive mutations, mutants refer to homozygotes of these mutations in this report. These mutations were classified into the following five phenotypic groups and features of these mutations were summarized in Table 1.

2.2.1. Mutations affecting liver morphogenesis

Mutations in four genes, *kakurembo* (*kak*), *hiohgi* (*hio*), *origami* (*ora*) and *kamifusen* (*kam*) affect liver morphology.

In live *kak* embryos at st. 34, the liver was not clearly discernible at the position where it should be formed and the gall bladder was dislocated anteriorly (Fig. 2A,B). In *kak* mutant embryos at st. 24, the expression level of *gata6* in the liver markedly reduced, while that of *cardiac myosin light chain* (*mlc*) in the heart was unaltered (Fig. 2G,H). In *kak* mutant embryos at st. 34, the expression level of *foxA3* was also greatly reduced (Fig. 2I,J). Since liver budding appeared to occur in *kak* mutants, *kak* may be required for the growth or maintenance of the liver. The gut tube was undulated at st. 36 (data not shown) without affecting the epithelial structure of the gut tube (Fig. 2N,O,Q,R).

In *hio* mutant embryos at st. 36 and at later stages, the liver was small and malformed (Fig. 2C,D, and data not shown). In situ hybridization using the *gata6* probe clearly showed impaired liver formation in *hio* mutant embryos at st. 30 (Fig. 2K,L). In addition to the liver defects, *hio* mutant embryos also lacked pectoral fins and died after hatching.

In *kam* mutant embryos, blood accumulated in the liver, and the liver was malformed (Fig. 2E). The expression of *gata6* appeared normal (Fig. 2M).

In *ora* mutant embryos at st. 36, the liver shape was altered, the gall bladder was displaced and the gut undulated (Fig. 2F). *ora* mutant embryos at st. 40 have an enlarged swim bladder and undulated gut, whereas the heart and kidneys appeared unaltered (Fig. 2T,U). Cross sections at the level of the liver, gut tube, and yolk showed that hepatocytes seemed normal, but the embryo itself lay apart from the yolk and the intestine was malformed (Fig. 2P,S). In contrast to regularly aligned polarized epithelial cells in

Table 1
Mutations affecting liver formation and function

Genes	Alleles	Viability	Phenotypes	Other phenotypes	References
Group 1: Mutations affecting liver morphogenesis					
kakurembo (kak)	*j140-3B*	Embryonic lethal	Small and mislocated liver	Mislocated gall bladder, undulated gut	
hiohgi (hio)	*j102-5B*	Embryonic viabe	Small liver	Fin missing	
kamifusen (kam)	*j124-4A*	Embryonic lethal	Malformed liver	Blood accumulated near the liver	
origami (ora)	*j137-1A*	Embryonic viable	Malformed liver	Undulated gut, enlarged swim bladder	
Group 2: Mutations affecting liver laterality					
kendama (ken)	*j103-11C*	Develop to adult fish	Inverted positions of liver and gall bladder	Medially located liver and missing spleen	
hanetsuki (hat)	*j68-7A*	Develop to adult fish	Inverted positions of liver and gall bladder	Inverted heart looping	
dendendaiko (den)	*j73-11A*	Develop to adult fish	Inverted positions of liver and gall bladder	Inverted heart looping	
Group 3: Mutations affecting bile color in the gall bladder					
akane (aka)	*j140-8A*	Embryonic lethal	Deep red bile	Colorless erythrocytes	
suou (suo)	*j98-5A*	Adult viable	Light red bile	Erythrocytes were faint red	
ominaeshi (omi)	*j24-13E*	Embryonic lethal	Colorless bile	Colorless erythrocytes	
Group 4: Mutations affecting lipid metabolism					
ukon (uko)	*j152-8A*	Embryonic lethal	Failure in metabolizing PED6	Edematic after hatching	a
aonibi (aon)	*j60-3A/j9-2F*	Embryonic lethal	Failure in metabolizing PED6	Small and degenerated forebrain at st. 38	
uguisucha (ugu)	*j153-9A*	Embryonic lethal	Failure in metabolizing PED6	Growth retardation after hatching	
Group 5: Mutations affecting endoderm formation					
akatsuki (aku)	*j22-15A/jf121-1A*	Embryonic lethal	Lacking *foxA3* expression	Similar to the zebrafish *oep* phenotype	a,b
akebono (ake)	*j54-7A*	Embryonic lethal	Lacking *foxA3* expression	Similar to the zebrafish *oep* phenotype	a,b
mochizuki (moc)	*j96-11B*	Embryonic lethal	Lacking *foxA3* expression	Similar to the zebrafish *oep* phenotype	a,b
sakura (sak)	*jr10-4A/j153-3A*	Embryonic lethal	Lacking the hepatic bud	Loss of heart and degeneration of eyes	b
hirame (hir)	*j54-20C*	Embryonic lethal	Defect in hypoblast convergence	Flat embryo	a,b
fukuwarai (fku)	*j8-33A/j93-4A*	Embryonic lethal	Lacking the hepatic bud	Cell polarity and alignment affected	a,b

References: a, Kitagawa et al., 2004; b, Furutani-Seiki et al., 2004.

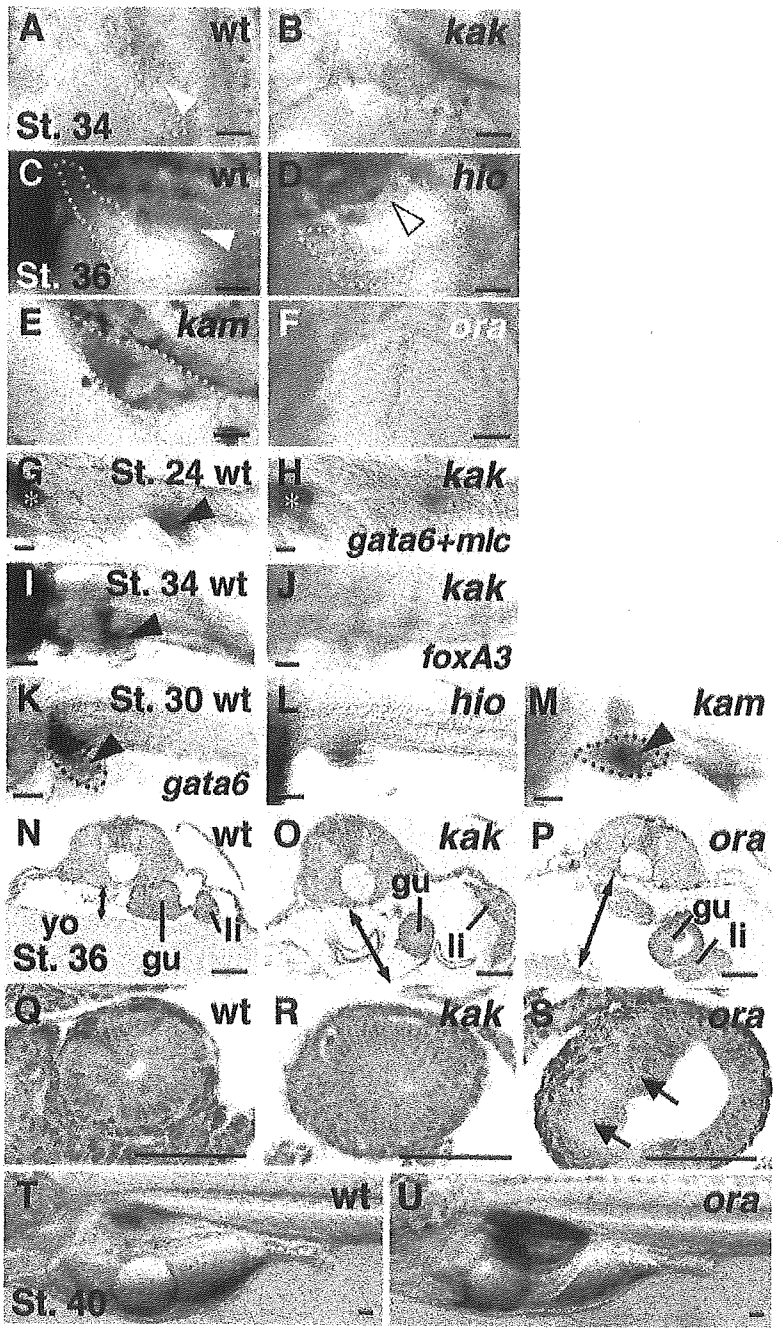

Fig. 2. *kak*, *hio*, *kam* and *ora* mutations affect liver morphogenesis. (A–F, T, and U) Live embryos; (G–M) Fixed embryos stained by in situ hybridization; (N–S) Histological sections stained with hematoxylin and eosin. in situ hybridization was performed using the probes of (G and H) *gata6* and *mlc*; (I and J) *foxA3*; and (K–M) *gata6*. (Q–S) Enlarged view of (N–P), respectively. (A–F, K–M, T and U) Lateral views, (G and H) dorsal views, anterior to the left, (N–S) Cross-sections. (A and B) st. 34; (C–F) st. 36; (G and H) st. 24; (I and J) st. 34; (K–M) st. 30; (N–S) st. 36; (T and U) st. 40. (A, C, G, I, K, N, Q, and T) Wild-type sibling embryos; (B, D, F, H, J, L, M, O, P, R, S, and U) Mutant embryos of (B, H, J, O, and R) *kak*; (D and L) *hio*; (E and M) *kam*; (F, P, S, and U) *ora*. Both arrows indicate the space between the yolk and the embryo proper. White broken lines demarcate the liver. Black and white arrowheads and white asterisks indicate the hepatic bud, gall bladder, and heart, respectively. Black arrows indicate the affected epithelial structure of the gut in the *ora* mutant. Gu: gut, Li: liver, yo: yolk. Scale bars correspond to 50 μm.

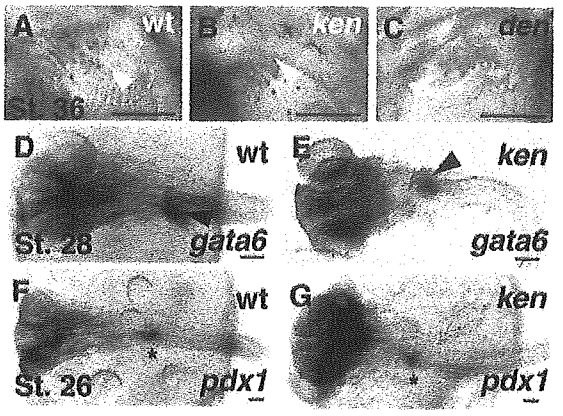

Fig. 3. *ken* and *den* mutations affect liver laterality. (A–C) Live embryos; (D–G) Embryos stained by in situ hybridization using the *gata6* (D and E) and *pdx1* (F and G) probes. (A–C) Lateral views, (D–G) dorsal views, (A, B, D–G) anterior to the left, (C) anterior to the right. (A and D) Wild-type sibling embryos; (B, C, E, and G) Mutant embryos, (B and E) *ken*, (C) *den* mutant embryos. White broken lines demarcate the livers. Black arrowheads, white arrowheads, and black asterisks indicate the liver, gall bladder, and pancreas, respectively. Scale bars correspond to 150 μm.

wild-type embryos, epithelial cells were irregularly arranged in *ora* mutant embryos (arrows in Fig. 2S).

2.2.2. *Mutations affecting liver laterality*

Mutations in three genes, *kendama* (*ken*), *dendendaiko* (*den*) and *hanetsuki* (*hat*), caused altered liver laterality (Fig. 3). In addition to the liver, the gall bladder, hepatic vein and blood vessels from the liver to the Cuvierian duct were also inverted in these mutant embryos. All mutant embryos hatched and their larvae swam well, suggesting that the altered laterality of the liver and other organs do not affect embryonic viability.

In *ken* mutant embryos, the laterality of the liver and heart was found to be uncoupled, as shown in Table 2. *ken* mutant embryos are classified into four groups according to the location of the liver and heart: (1) the liver shifts to the center and the heart is normally located, L(c)H(n); (2) the liver shifts to the center and the heart was inverted, L(c)H(i); (3) the liver shifts to the right with the heart normally positioned, L(r)H(n); (4) the liver shifts to the right and the heart was inverted, L(r)H(i). These phenotypes were observed in subsequent generations. A *ken* mutant embryo of L(c)H(n) at st. 36 is shown in Fig. 3B. In the embryo in which the liver and gall bladder were located at the center of the body, the liver was not visible from the left view but the heart was observed at the normal location (data not shown). Since, in Medaka the pancreas, detected by the expression of *pdx1*, lies at the center of embryos in the wild-type embryo at st. 26 (Assouline et al., 2001), we could not determine the laterality of the pancreas in *ken* mutant embryos (Fig. 3F,G).

In *den* and *hat* mutant embryos, the liver, gall bladder, and the heart were all inverted in these mutants, as shown in Fig. 3C and Table 2. These results suggest that while *den* and *han* are required for the general laterality of the body, *ken* is required for coupling the laterality of the liver and heart.

2.2.3. *Mutations affecting color of bile in the gall bladder*

Mutations in three genes, *suou* (*suo*), *akane* (*aka*) and *ominaeshi* (*omi*), affected the color of bile in the gall bladder (Fig. 4). Bile in the wild-type embryo at st. 35 was light green, as shown in Fig. 4A. The bile colors in the three mutants, *suo*, *aka* and *omi*, were orange, deep red and white, respectively (Fig. 4B–D). *aka* and *omi* mutant embryos were embryonic lethal, but *suo* mutant embryos hatched and *suo* homozygotes were fertile.

To determine whether these mutations affect either erythropoiesis or hemoglobin-bile metabolism, we first carried out hemoglobin staining with *o*-dianisidine. As shown in Fig. 4E–H, the blood vessels and heart, but not the gall bladder, were stained in *suo* mutant embryos, but were not stained in *aka* and *omi* mutant embryos. We next examined the expression of *globin* genes by in situ hybridization. Medaka embryos express three types of *globin*, *α-0*, *α-1*, and *β-1* (Maruyama et al., 2002). *α-0*, *α-1*, and *β-1 globins* were expressed in *suo* mutants at st. 33 (Fig. 4I,J,M,N, and data not shown), whereas *α-0*, but not *α-1* and *β-1 globins* were expressed in *aka* mutant embryos (Fig. 4K,O, and data not shown). None of *α-0*, *α-1*, and *β-1 globins* were expressed in *omi* mutant embryos (Fig. 4L,P, and data not shown). These results indicate that *aka* and *omi* mutations affect erythropoiesis. On the other hand,

Table 2
Frequency of alteration of liver and heart laterality

		Laterality phenotype (%)						
		Total	L(l) H(n)	L(l) H(i)	L(c) H(n)	L(c) H(i)	L(r) H(n)	L(r) H(i)
ken	mut	39	0	0	10 (26)	16 (40)	3 (7)	10 (26)
	sib	102	101 (99)	1 (1)	0	0	0	0
hat	mut	21	0	0	0	0	0	21 (100)
	sib	96	95 (99)	1 (1)	0	0	0	0
den	mut	19	0	0	0	0	1 (6)	18 (94)
	sib	120	119 (99)	1 (1)	0	0	0	0

L, liver; H, heart; l, left; c, center; r, right; n, normal; i, invert.

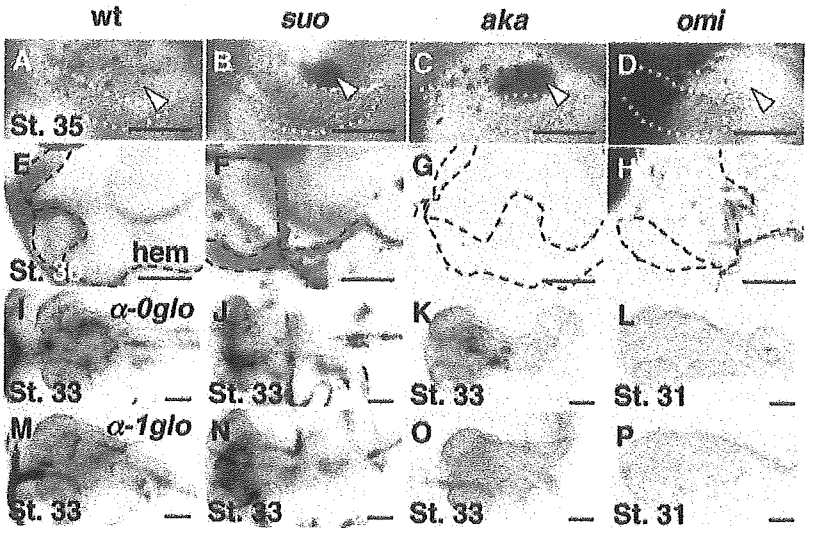

Fig. 4. *aka*, *suo* and *omi* mutations affect bile color. (A–D) Live embryos; (E–H) Hemoglobin staining; (I–P) in situ hybridization, using (I–L) the *α-0 globin*, and (M–P) *α-1 globin* probes. (A–D) st. 35; (E–H) st. 36; (I–K, M–O) st. 33 and (L and P) st. 31. (A, E, I, and M) wild-type sibling embryos, (B, F, J, and N) *suo*, (C, G, K, and O) *aka* and (D, H, L, and P) *omi* mutant embryos. White arrowheads and white broken lines indicate the gall bladder and margin of the liver, respectively. Black broken lines show the Cuvierian duct. Black to brownish spots are melanophores on the yolk. Scale bars correspond to 200 μm.

erythropoiesis appears normal and orange bile in the gall bladder is not due to the accumulation of erythrocytes in *suo* mutant embryos, suggesting that *suo* mutation may affect hemoglobin–bilirubin metabolism.

2.2.4. Mutations affecting lipid metabolism

The fluorescence intensities of PED6 metabolites markedly decreased in three mutant embryos, *ukon* (*uko*), *aonibi* (*aon*) and *uguisucha* (*ugu*), at st. 35 (Fig. 5C–F). To examine whether the decrease in fluorescence intensity is due to the inability of swallowing PED6, we loaded the three mutant embryos with BODIPY-FL-C5, an unquenched form of PED6. All the mutants swallowed the unquenched form of PED6, and the gut, liver and gall bladder showed fluorescence as wild-type embryos (Fig. 5G–J).

uko and *aon* mutant embryos appeared normal in the morphologies of the liver, gall bladder and intestine at st. 35 as shown in Fig. 5B, and *ugu* mutant embryos started to show retardation in development from st. 35 (data not shown). *uko* mutant embryos could hatch but their larvae died a few days after hatching (data not shown). Both *aon* and *ugu* mutant embryos were embryonic lethal. The forebrain was reduced in size from st. 23 in *aon* mutant embryos (Kitagawa et al., 2004). These results suggest that the *uko*, *aon* and *ugu* genes are required for the metabolism or transport of lipids in the hepatobiliary system.

2.2.5. Mutations affecting patterning of endoderm

Six mutations affecting formation of the endodermal rod and/or hepatic bud were identified. Mutations in the *fukuwarai* (*fku*) genes affected endodermal rod morphogenesis (Fig. 6G). Although in *fku* mutant embryos *foxA3* was expressed in the pharynx, hepatic region and the gut (Fig. 6, open circle, arrow head and asterisk, respectively), parts of the endodermal rod were randomly dislocated (Fig. 6G arrow) as other epithelial structures, such as the head structures originated from neuroepithelium (Fig. 6B closed arrow, Kitagawa et al., 2004).

In *sakura* (*sak*) mutant embryos, *foxA3* was expressed in the gut and hepatic region, but not in the pharynx (Fig. 6H). Growth of the hepatic region appeared to be affected and anterior part of the endodermal rod may be missing or misspecified. In *sak* mutant embryos, the heart was not formed and the eyes became degenerated at st. 28 (Fig. 6C, closed arrow).

In embryos with mutations in three genes, *akatsuki* (*aku*), *akebono* (*ake*) and *mochizuki* (*moc*), the endodermal rod was missing (Fig. 6I, data not shown). These mutants exhibited a body patterning phenotypes similar to those of *one-eyed-pinhead* (*oep*) zebrafish mutants (Fig. 6D, data not shown, Kitagawa et al., 2004). While embryos with mutations in only one gene exhibit the *oep* mutant phenotypes, those in three genes display similar phenotypes in both body patterning and endoderm formation.

In *hirame* (*hir*) mutant embryos, *foxA3* expressing endodermal cells did not converge properly, affecting the endermal rod formation (Fig. 6J open arrow). *hir* mutant embryos were flat and tissues such as the lens and heart were mislocated (Fig. 6E, the closed arrow indicates mislocated lens, Kitagawa et al., 2004).

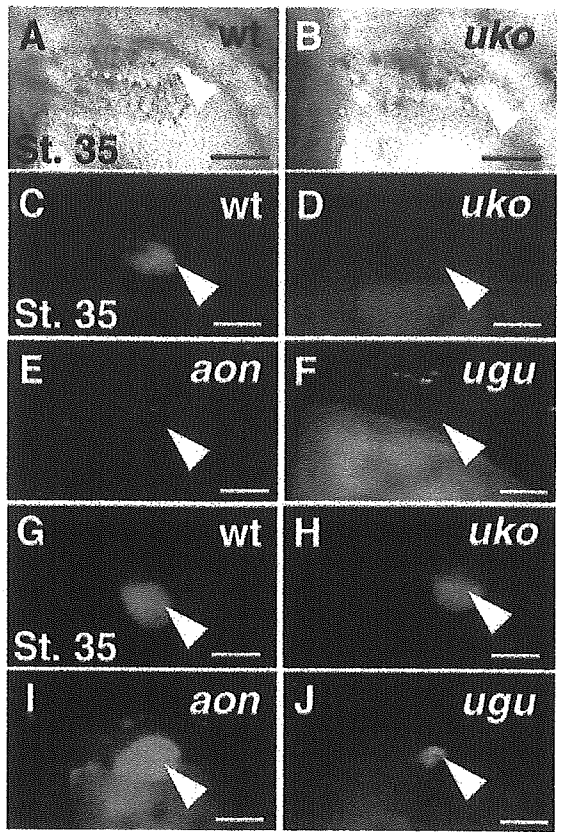

Fig. 5. *uko*, *ugu*, and *aon* mutations affect lipid metabolism. Laterl view, anterior to the left. Live embryos of unstained (A, B), stained with PED6 (C–F) and BODIPY FL-C5 (G–J) at st. 35. (A, C, and G) Wild-type, (B, D, and H) *uko*, (E and I) *aon* and (F and J) *ugu*. Metabolized PED6 (C-F) or BODIPY FL-C5 (G–J) can been seen as a green emission (Em: 505 nm) in the gall bladder (white arrowheads). White broken lines demarcate the margin of the liver. Scale bars correspond to 200 μm.

3. Discussion

3.1. Screening for mutations affecting liver development in Medaka

Partly due to the functional overlap of genes, particularly in vertebrates, mutagenesis screens in a single species are unlikely to be sufficient for identifying all essential genes involved in a particular biological process Therefore, mutagenesis screens and analyses of Medaka mutants complement those in zebrafish, in identifying a wider repertoire of genes by a forward genetic approach in vertebrates.

Our mutagenesis screen in Medaka identified mutations in 19 genes affecting various aspects of the development of the liver and associated tissues. These mutations are classified into five groups: (1) mutations affecting liver morphogenesis; (2) mutations affecting liver laterality; (3) mutations affecting of bile color; (4) mutations affecting lipid metabolism; and (5) mutations affecting endoderm and hepatic bud formation. In zebrafish, a mutagenesis screen using GFP-transgenic fish, whose developing endoderm or organs arising from endoderm are more conspicuous, is underway (D. Y. R. Stainier, personal communication). Thus, mutagenesis screens in both Medaka and zebrafish should be complementary in identifying conserved and divergent mechanisms of liver development.

In our screen, we initially aimed to identify mutations affecting formation and function of the liver specifically. To this end we carried out a screen by multiple criteria to reveal the specificity of the defect. Majority of mutations that we identified were those affecting tissues in addition to the liver during development. From these results, we deduced that mutations affecting the liver specifically may be very limited and that even if defects are not confined to the liver, mutated genes are important for the formation of the liver or physiological functions in which the liver is involved. Thus expression of these genes identified in our screen may not be restricted to the liver but to the tissues, from which the liver originates or those working with the liver to exert its physiological functions.

3.2. Mutations affecting liver morphogenesis

Several explanations may account for the phenotypes of Group 1 mutants with defects in the liver, and gall bladder and gut. First, cell-autonomous defects may affect the regional morphogenesis of the endodermal rod, resulting in altered morphologies of the liver, gall bladder and gut. Second, non-cell-autonomous defects such as the interaction between the surrounding lateral mesoderm and endodermal rod may cause the phenotype. Third, there may be regulatory interactions among the hepatic bud, primordium of the gall bladder and the intestinal bulb. Transplantation experiments to determine the cell autonomy of these mutations would be useful to clarify these possibilities. Finally, since nutrients absorbed from the intestine are metabolized in the liver (Wallace and Pack, 2003; Warga and Stainier, 2002), a defect in the intestine may affect liver growth. The idea that the timing of liver growth is dependent on nourishment from the intestine needs to be further investigated.

In *kak* mutants, although the hepatic bud is formed, the liver is very small at st. 34 and the gall bladder may have shifted its position due to the small liver. This suggests that *kak* is required for the formation of the liver from the hepatic bud.

In *hio* mutants, the liver is small and malformed and the pectoral fin is missing. In zebrafish, some mutations affect the pectoral fin, but no mutations have been reported to affect both the liver and pectoral fin yet (Grandel and Schulte-Merker, 1998; Neumann et al., 1999; van Eeden et al., 1996). It has been suggested that, however, mesodermal components or FGF signaling is

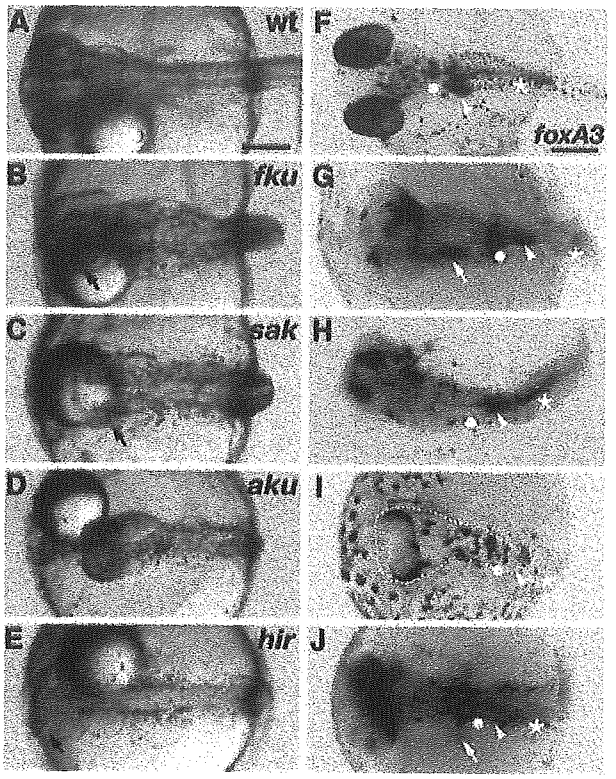

Fig. 6. *fku, sak, aku,* and *hir* mutations affect patterning of endoderm. Dorsal views of (A–E) live embryos and (F–J) embryos stained by in situ hybridization using the *foxA3* probe at st. 28. (A and F) Wild-type embryos, (B and G) *fku*; (C and H) *sak*, (D and I) *aku* and (E and J) *hir* mutant embryos. Open circle, arrowhead, and asterisk indicate the sites where pharynx, hepatic bud, and the gut are normally formed, respectively. Closed arrows show dislocated head structure in B, degenerating eye in C, dislocated lens in E. Open arrows indicate mislocated part of the endodermal rod in G and *foxA3* positive cells inappropriately converged in J. The margin of the embryo was demarcated by the broken line in I. Scale bars correspond to 250 μm.

required for the formation of the pectoral fin and liver (Fischer et al., 2003; Jung et al., 1998; Martin, 1998). It would be interesting to examine mesoderm development and FGF expression in *hio* mutant embryos to further characterize this mutation.

In *kam* mutant embryos, in addition to a malformed liver and gall bladder, the heart is small and blood accumulates near the liver and gut. Such blood accumulation may reflect a defect either in vasculature formation in the liver or in endothelial cell development. In *vegfr2/flk-1* mutant mice with endothelial cell defects, liver budding does not occur. However, in zebrafish, although *cloche* zebrafish mutants lacking all endothelial cells, normal liver budding and development occurs (Field et al., 2003; Stainier et al., 1995). However, severe cardiac edema did not allow analysis of the requirement of endothelial cells during the growth of the liver in those studies. In *kam* mutants, liver budding seems to occur normally, but the growth of the liver may be affected. Detailed analysis of *kam* mutants at the budding and growth periods using endothelial markers would be useful for the further characterization of this mutation.

3.3. Laterality of the liver and other organs

The laterality of all the organs is inverted in most of mutants of zebrafish and mice (Essner et al., 2000; Faucourt et al., 2001; Mochizuki et al., 2002; Schilling et al., 1999), but there are a few reports on uncoupled laterality of the organs (Bisgrove et al., 2000; Field et al., 2003). In zebrafish *flh* and *boz* mutants, the laterality of the liver and heart is randomized and uncoupled (Chin et al., 2000). *flh* is required for specification of the chordamesoderm and *boz* is required for dorsal axis formation. Both *flh* and *boz* are required for early specification of the notochord. Collectively, *ken* mutants show a defect in the laterality of the viscera as observed in *flh* and *boz* mutants but do not show other morphological deficits. An interesting possibility is that *ken* might be a component of the signaling downstream of *boz* and *flh*.

3.4. Mutations affecting bile color

Since a compromised function of the liver readily results in jaundice in human, hemoglobin metabolism producing bilirubin is one of the most important functions of the liver

Hereditary diseases affecting bilirubin metabolism are known in human (Nowicki and Poley, 1998).

Mutations affecting the color of bile in the gall bladder and red blood cells were identified in zebrafish (Ransom et al., 1996; Shafizadeh et al., 2002; Thisse and Zon, 2002; Weistein et al., 1996). *aka* and *omi* mutations also affect erythropoiesis in Medaka. In contrast, *suo* mutation seems to be the first mutation affecting hemoglobin–bilirubin metabolism in zebrafish and Medaka. It would be of interest if *suo* mutation models a human disease.

3.5. Lipid metabolism

PED6 is a substrate for PLA_2 cleavage and a sensitive reporter of its enzymatic activity in vivo (Farber et al., 2001). PLA_2 is important in the generation of lipid signaling molecules, host defenses, lipid absorption and cancer. It is thus a good chemical reagent for screening mutations affecting lipid metabolism. Using PED6, four mutations affecting digestive organ morphology and one mutation affecting bile synthesis or secretion were identified in zebrafish (Farber et al., 2001).

The *uko, aon,* and *ugu* mutations may affect steps in the lipid metabolism pathway, such as ingestion and cleavage of the lipid within the intestine, and subsequent hepatobiliary transport to the gall bladder (Faber et al., 2001). Further biochemical characterization is necessary to determine which component of lipid metabolism is affected in Group 4 mutants.

3.6. Mutations affecting endoderm formation and patterning

The phenotypes of *aku, ake* and *moc* mutants in patterning of the body, endoderm and mesoderm, are similar to those of zebrafish *oep* mutants with defects in the Nodal signaling pathway (Schier et al., 1996, 1997; Zhang et al., 1998). Zebrafish mutations in other components of the Nodal signaling pathway, such as *cyclops, squint* and *smalspur*, exhibit phenotypes substantially different from that of *oep* mutation (Brand et al., 1996). Cloning of three genes, *aku, ake* and *moc* genes will clarify the conserved or divergent functions of these genes in endoderm specification.

The *fku* and *hir* mutants show unique phenotypes in the patterning of the body, not recorded yet in the collection of zebrafish mutants. In *fku* mutants, parts of the head, such as the eyes and nose, are mislocated. In *hir* mutants, the body becomes thinner and several tissues, such as the lens and heart, are mislocated. Although the endodermal cells expressing *foxA3* are present, morphogenesis of the hepatic bud and convergence of the endodermal cells did not occur properly in *fku* and *hir* mutants, respectively. Interestingly, the common feature between *fku* and *hir* mutants is the marked defect of cell alignment in the epithelium (Furutani-Seiki et al., unpublished results). Further analysis of *fku* and *hir* mutants using early hepatocyte markers may help clarify the relationship between endodermal epithelialization and morphogenesis or specification of the endodermal rod.

In *sak* mutants, the heart primordium and the anterior part of the endodermal rod are not formed. It has been reported that the cardiac mesoderm is necessary for the induction of hepatic bud in mice (Duncan, 2003; Jung et al., 1999; Rossi et al., 2001). Further investigation of the requirement of *sak* in the heart or liver by transplantation experiments may provide insights into tissue interactions in heart and liver development.

4. Experimental procedures

4.1. Maintenance of fish stocks

Fish maintenance and mating were carried out as described elsewhere (Furutani-Seiki et al., 2004). Briefly, the Kyoto-Cab sub-strain and Kaga strain were used to induce mutations in the male germline by treatment with ENU (Ethyl-Nitroso-Urea). F3 progenies homozygous for induced mutations were generated by a three generation incrossing scheme.

4.2. Screening procedures

Live F3 progenies were screened for developmental defects at st. 32 and 36 using a Leica MZ12.5 dissecting microscope. For functional screening, we used PED6, a fluorescent PLA_2-substrate dye. PLA_2 cleavage liberates the BODIPY-acyl chain of PED6, resulting in unquenching and green fluorescent emission as described previously (Farber et al., 2001). As the control, BODIPY FL-C5, an unquenched form of PED6 was used. Embryos at st. 35 were placed in 0.5 ml of 1 × Balanced Salt Solution (BSS; 110 mM NaCl, 5 mM KCl, 1 mM $CaCl_2$, and 2.2 mM $MgSO_4$, pH 7.2), containing 0.3 μg/ml PED6 or 0.2 μg/ml BODIPY-FL-C5, and incubated in the dark for 4 h at 28 °C. The embryos were then rinsed with 1 × BSS and placed in a glass depression slide. Using a Zeiss Axioplan 2 microscope, samples were examined for fluorescence from PED6 or BODIPY-FL-C5.

4.3. Histological sections

Embryos were dechorionated and fixed in 4% paraformaldehyde in PBS(−) overnight at 4 °C. The embryos were dehydrated with ethanol and stored at −20 °C. For sectioning, they were incubated in xylene and embedded in paraffin at 67 °C. Paraffin embedded embryos were sectioned (4 μm thickness) and stained with hematoxylin and eosin.

4.4. In situ hybridization

Whole mount in situ hybridization was performed as described elsewhere (Sasado et al., 2004), using an

anti-sense DIG-labeled riboprobe generated from Medaka *foxA3*, *gata6*, *mlc*, *pdx1*, *α-0*, *α-1*, and *β-1 globin* cDNA. Dechorionated embryos were fixed with 4% paraformaldehyde and 0.1% Tween 20 in PBS(−). Embryos later than st. 30 were treated with proteinase K and to remove pigmentation, with H_2O_2. Embryos were photographed using a Leica dissecting microscope.

4.5. Whole embryo staining for hemoglobin expression

Hemoglobin staining was done as described previously (Cocca et al., 1995). Dechorionated embryos were stained for 15 min in the dark in *o*-dianisidine (0.6 mg/ml), 0.01 M sodium acetate (pH 4.5), 0.65% H_2O_2 and 40% (vol/vol) ethanol. Stained embryos were cleared with benzyl benzoate/benzyl alcohol (2:1, vol/vol) and examined with a dissecting microscope.

Acknowledgements

We are grateful to Drs Takashi Sasaki and Noboru Nakajima for cloning *gata6* and *foxA3* probes, Dr Raphael Scharfmann for the *pdx1* probe and to Haruka Momose and Takahiro Negishi for in situ hybridization and graphical works. We would like to thank Drs Shuji Terai and Kiwamu Okita for continual discussion and encouragement. This work was supported by the ERATO project of the Japan Science and Technology Agency to H.K.

References

Alexander, J., Stainier, D.Y., 1999. A molecular pathway leading to endoderm formation in zebrafish. Curr. Biol. 9, 1147–1157.

Assouline, S., Nir, S., Lahav, N., 2001. Simulation of non-enzymatic template-directed synthesis of oligonucleotides and peptides. J. Theor. Biol. 208, 117–125.

Bisgrove, B.W., Essner, J.J., Yost, H.J., 2000. Multiple pathways in the midline regulate concordant brain, heart and gut left-right asymmetry. Development 127, 3567–3579.

Brand, M., Heisenberg, C.P., Warga, R.M., Pelegri, F., Karlstrom, R.O., Beuchle, D., Picker, A., Jiang, Y.J., Furutani-Seiki, M., van Eeden, F.J., Granato, M., Haffter, P., Hammerschmidt, M., Kane, D.A., Kelsh, R.N., Mullins, M.C., Odenthal, J., Nusslein-Volhard, C., 1996. Mutations affecting development of the midline and general body shape during zebrafish embryogenesis. Development 123, 129–142.

Chen, J.N., Haffter, P., Odenthal, J., Vogelsang, E., Brand, M., van Eeden, F.J., Furutani-Seiki, M., Granato, M., Hammerschmidt, M., Heisenberg, C.P., Jiang, Y.J., Kane, D.A., Kelsh, R.N., Mullins, M.C., Nusslein-Volhard, C., 1996. Mutations affecting the cardiovascular system and other internal organs in zebrafish. Development 123, 293–302.

Chin, A.J., Tsang, M., Weinberg, E.S., 2000. Heart and gut chiralities are controlled independently from initial heart position in the developing zebrafish. Dev. Biol. 227, 403–421.

Cocca, E., Ratnayake-Lecamwasam, M., Parker, S.K., Camardella, L., Ciaramella, M., di Prisco, G., Detrich, H.W., 1995. Genomic remnants of alpha-globin genes in the hemoglobinless antarctic icefishes. Proc. Natl Acad. Sci. USA 92, 1817–1821.

Douarin, N.M., 1975. An experimental analysis of liver development. Med. Biol. 53, 427–455.

Duncan, S.A., 2003. Mechanisms controlling early development of the liver. Mech. Dev. 120, 19–33.

Essner, J.J., Branford, W.W., Zhang, J., Yost, H.J., 2000. Mesendoderm and left-right brain, heart and gut development are differentially regulated by pitx2 isoforms. Development 127, 1081–1093.

Farber, S.A., Pack, M., Ho, S.Y., Johnson, I.D., Wagner, D.S., Dosch, R., Mullins, M.C., Hendrickson, H.S., Hendrickson, E.K., Halpern, M.E., 2001. Genetic analysis of digestive physiology using fluorescent phospholipid reporters. Science 292, 1385–1388.

Faucourt, M., Houliston, E., Besnardeau, L., Kimelman, D., Lepage, T., 2001. The pitx2 homeobox protein is required early for endoderm formation and nodal signaling. Dev. Biol. 229, 287–306.

Field, H.A., Ober, E.A., Roeser, T., Stainier, D.Y., 2003. Formation of the digestive system in zebrafish. I. Liver morphogenesis. Dev. Biol. 253, 279–290.

Fischer, S., Draper, B.W., Neumann, C.J., 2003. The zebrafish fgf24 mutant identifies an additional level of Fgf signaling involved in vertebrate forelimb initiation. Development 130, 3515–3524.

Furutani-Seiki, M., Sasado, T., Morinaga, C., Suwa, H., Niwa, K., Yoda, H., et al., 2004. A systematic genome-wide screen for mutations affecting organogenesis in Medaka, *Oryzias latipes*. Mech. Dev. 121, 647–658.

Grandel, H., Schulte-Merker, S., 1998. The development of the paired fins in the zebrafish (Danio rerio). Mech. Dev. 79, 99–120.

Grapin-Botton, A., Melton, D.A., 2000. Endoderm development: from patterning to organogenesis. Trends Genet. 16, 124–130.

Jung, J., Zheng, M., Goldfarb, M., Zaret, K.S., 1999. Initiation of mammalian liver development from endoderm by fibroblast growth factors. Science 284, 1998–2003.

Kitagawa, D., Watanabe, T., Saito, K., Asaka, S., Sasado, T., Morinaga, C., et al., 2004. Genetic dissection of the formation of the forebrain in Medaka, *Oryzias latipes*. Mech. Dev. 121, 673–685.

Martin, G.R., 1998. The roles of FGFs in the early developments of vertebrate limbs. Genes Dev. 12, 1571–1586.

Maruyama, K., Yasumasu, S., Iuchi, I., 2002. Characterization and expression of embryonic and adult globins of the teleost *Oryzias latipes* (medaka). J. Biochem. 132, 581–589.

Matsumoto, K., Toshitomi, H., Rossant, J., Zaret, K.S., 2001. Liver organogenesis promoted by endothelial cells prior to vascular function. Science 294, 559–563.

Mochizuki, T., Tsuchiya, K., Yokoyama, T., 2002. Molecular cloning of a gene for inversion of embryo turning (inv) with cystic kidney. Nephrol. Dial. Transplant 17(Suppl. 9), 68–70.

Neumann, C.J., Grandel, H., Gaffield, W., Schulte-Merker, S., Nusslein-Volhard, C., 1999. Transient establishment of anteroposterior polarity in the zebrafish pectoral fin bud in the absence of sonic hedgehog activity. Development 126, 4817–4826.

Nishina, H., Vaz, C., Billia, P., Nghiem, M., Sasaki, T., De la Pompa, J.L., Furlonger, K., Paige, C., Hui, C., Fischer, K.D., Kishimoto, H., Iwatsubo, T., Katada, T., Woodgett, J.R., Penninger, J.M., 1999. Defective liver formation and liver cell apoptosis in mice lacking the stress signaling kinase SEK1/MKK4. Development 126, 505–516.

Nowicki, M.J., Poley, J.R., 1998. The hereditary hyperbilirubinaemias. Baillieres Clin. Gastroenterol. 12, 355–367.

Ober, E.A., Field, H.A., Stainier, D.Y., 2003. From endoderm formation to liver and pancreas development in zebrafish. Mech. Dev. 120, 5–18.

Pack, M., Solnica-Krezel, L., Malicki, J., Neuhauss, S.C., Schier, A.F., Stemple, D.L., Driever, W., Fishman, M.C., 1996. Mutations affecting development of zebrafish digestive organs. Development 123, 321–328.

Ransom, D.G., Haffter, P., Odenthal, J., Brownlie, A., Vogelsang, E., Kelsh, R.N., Brand, M., van Eeden, F.J., Furutani-Seiki, M., Granato, M., Hammerschmidt, M., Heisenberg, C.P., Jiang, Y.J., Kane, D.A., Mullins, M.C., Nusslein-Volhard, C., 1996. Characterization of zebrafish mutants with defects in embryonic hematopoiesis. Development 123, 311–319.

Rossi, J.M., Dunn, N.R., Hogan, B.L., Zaret, K.S., 2001. Distinct mesodermal signals, including BMPs from the septum transversum

mesenchyme, are required in combination for hepatogenesis from the endoderm. Genes Dev. 15, 1998–2009.
Sasado, T., Morinaga, C., Niwa, K., Shinomiya, A., Yasuoka, A., Suwa, H., et al., 2004. Mutations affecting early distribution of primordial germ cells in Medaka (*Oryzias latipes*) embryo. Mech. Dev. 121, 817–828.
Schier, A.F., Neuhauss, S.C., Harvey, M., Malicki, J., Solnica-Krezel, L., Stainier, D.Y., Zwartkruis, F., Abdelilah, S., Stemple, D.L., Rangini, Z., Yang, H., Driever, W., 1996. Mutations affecting the development of the embryonic zebrafish brain. Development 123, 165–178.
Schier, A.F., Neuhauss, S.C., Helde, K.A., Talbot, W.S., Driever, W., 1997. The one-eyed pinhead gene functions in mesoderm and endoderm formation in zebrafish and interacts with no tail. Development 124, 327–342.
Schilling, T.F., Concordet, J.P., Ingham, P.W., 1999. Regulation of left-right asymmetries in the zebrafish by Shh and BMP4. Dev. Biol. 210, 277–287.
Shafizadeh, E., Paw, B.H., Foott, H., Liao, E.C., Barut, B.A., Cope, J.J., Zon, L.I., Lin, S., 2002. Characterization of zebrafish merlot/chablis as non-mammalian vertebrate models for severe congenital anemia due to protein 4.1 deficiency. Development 129, 4359–4370.
Stainier, D.Y., Weinstein, B.M., Detrich, H.W. 3rd, Zon, L.I., Fishman, M.C., 1995. Cloche, an early acting zebrafish gene, is required by both the endothelial and hematopoietic lineages. Development 121, 3141–3150.
Tam, P.P., Kanai-Azuma, M., Kanai, Y., 2003. Early endoderm development in vertebrates: lineage differentiation and morphogenetic function. Curr. Opin. Genet. Dev. 13, 393–400.
Thisse, C., Zon, L., 2002. Organogenesis-heart and blood formation from the zebrafish point of view. Science 295, 457–462.
van Eeden, F.J., Granato, M., Schach, U., Brand, M., Furutani-Seiki, M., Haffter, P., Hammerschmidt, M., Heisenberg, C.P., Jiang, Y.J., Kane, D.A., Kelsh, R.N., Mullins, M.C., Odenthal, J., Warga, R.M., Nusslein-Volhard, C., 1996. Genetic analysis of fin formation in the zebrafish. Danio rerio. Development 123, 255–262.
Wada, T., Joza, N., Cheng, H.M., sasaki, T., Kozieradzki, I., Bachmaier, K., Katada, T., Schreiber, M., Wagner, E.F., Nishina, H., Penninger, J.M., 2004. MKK7 couples stress signaling to G2/M cell cycle progression and cellular senescence. Nat. Cell Biol. 6, 215–226.
Wallace, K.N., Pack, M., 2003. Unique and conserved aspects of gut development in zebrafish. Dev. Biol. 255, 12–29.
Warga, R.M., Stainier, D.Y., 2002. The guts of endoderm formation. Results Probl. Cell Differ. 40, 28–47.
Watanabe, T., Nakagawa, K., Ohata, S., Kitagawa, D., Nishitai, G., Seo, J., Tanemura, S., Shimizu, N., Kishimoto, H., Wada, T., Aoki, J., Arai, H., Iwatsubo, T., Mochita, M., Satake, M., Ito, Y., Matsuyama, T., Mak, T.W., Penninger, J.M., Nishina, H., Katada, T., 2002. SEK1/MKK4-mediated SAPK/JNK signaling participates in embryonic hepatoblast proliferation via a pathway different from NF-κB-induced anti-apoptosis. Dev. Biol. 250, 332–347.
Weistein, B., Schier, A., Abdelilar, S., Malicki, J., Solnica-Krezel, L., Stemple, D., Stainier, D.Y., Zwartkruis, F., Driever, W., Fishman, M., 1996. Hematopoietic mutations in the zebrafish. Development 123, 303–309.
Zaret, K.S., 2001. Hepatocyte differentiation: from the endoderm and beyond. Curr. Opin. Genet. Dev. 11, 568–574.
Zaret, K.S., 2002. Regulatory phases of early liver development: paradigms of organogenesis. Nat. Rev. Genet. 3, 499–512.
Zhang, J., Talbot, W.S., Schier, A.F., 1998. Positional cloning identifies zebrafish one-eyed pinhead as a permissive EGF-related ligand required during gastrulation. Cell 92, 241–251.

Glossary

hiohgi:	a traditional Japanese hand fan for court functions;
kakurembo:	a game of hide-and-seek;
kamifusen:	a balloon made of paper;
origami:	art of folding paper;
kendama:	Japanese toy with a wooden cup and a ball on a thread, where one tries to catch the ball in the cup;
hanetsuki:	traditional Japanese badminton using colored wooden racquets and a shuttlecock;
dendendaiko:	a Japanse drum for children that makes a sound by turning it upside down;
akane, suou:	traditional Japanese term for red;
ominaeshi:	a traditional Japanese term for white;
uguisucha, ukon:	traditional Japanese dark yellow color;
aonibi:	dark green;
fukuwarai:	Japanese jigsaw-puzzle to make with face blindfolded;
sakura:	cherry blossom;
akebono:	rising sun;
akatsuki, mochizuki:	full moon;
hirame:	flounder

JB Minireview

J. Biochem. **136**, 00–00 (2004)
DOI: 10.1093/jb/mvh117

Physiological Roles of SAPK/JNK Signaling Pathway

Hiroshi Nishina*, Teiji Wada and Toshiaki Katada

Department of Physiological Chemistry, Graduate School of Pharmaceutical Sciences, University of Tokyo, Tokyo 113-0033

Received May 6, 2004; accepted May 6, 2004

Stress-activated protein kinase/c-Jun NH_2-terminal kinase (SAPK/JNK) is activated by many types of cellular stresses and extracellular signals. Recent studies, including the analysis with knockout mice, have led to progress towards understanding the physiological roles of SAPK/JNK activation in embryonic development in addition to immune responses. SAPK/JNK activation plays essential roles in organogenesis during mouse development by regulating cell survival, apoptosis, and proliferation. Two SAPK/JNK activators, SEK1 and MKK7, are required for fetal liver formation and full activation of SAPK/JNK, which responds to various stimuli in an all-or-none manner. This article focuses on physiological roles of SAPK/JNK activation in fetal liver formation and in apoptosis regulation.

Key words: apoptosis, liver formation, MAP kinase, SAPK/JNK, stress.

Developmental programs and environmental agents trigger distinct and evolutionarily conserved kinases that relay signals mediating survival, death, proliferation, and cell cycle arrest. Mitogen-activated protein kinases (MAPKs) are evolutionarily conserved serine/threonine kinases involved in regulation of many cellular events. Several MAPK groups have been identified in mammalian cells, including extracellular signal-regulated kinase (ERK), p38, and SAPK/JNK. These MAPKs are activated by their specific MAPK kinases (MAPKKs): ERK by MEK1 and MEK2, p38 by MKK3 and MKK6, and SAPK/JNK by SEK1 (also known as MKK4) and MKK7 (SEK2). These MAPKKs are also activated by various MAPKK kinases (MAPKKKs) such as Raf, MLK, MEKK1, TAK1, and ASK1.

SAPK/JNK is ubiquitously expressed and is activated by many types of stress, including UV and γ-irradiation, protein synthesis inhibitors (anisomycin), hyperosmolarity, toxins, ischemia/reperfusion injury in heart attacks, heat shock, anticancer drugs (cisplatinum, adriamycin, or etoposide), ceramide, T-cell receptor stimulation, peroxide, and inflammatory cytokines such as TNFα. Recently, several *in vitro* and *in vivo* experiments have shown that SAPK/JNK is activated synergistically by SEK1 and MKK7. The SAPK/JNK stress pathway participitates in many different intracellular signaling pathways that control a spectrum of cellular processes, including cell proliferation, differentiation, transformation, apoptosis, migration, and cytoskeletal integrity. SAPK/JNK has been reported to phosphorylate transcription factors in addition to c-Jun, such as ATF-2, Elk-1, p53, and c-Myc, as well as nontranscription factors such as Bcl-2, Bcl-xL, paxillin, and MAP2 (*1–6*). This review summarizes recent progress in the SAPK/JNK signaling pathway in mouse development and the molecular mechanism of SAPK/JNK activation.

*To whom correspondence should be addressed. Tel: +81-3-5841-4754, Fax: +81-3-5841-4751, E-mail: nishina@mol.f.u-tokyo.ac.jp

Role of SAPK/JNK in mouse development

All three *Jnk* (*Jnk1*, *2*, and *3*), and *sek1* and *mkk7* loci have been knocked out. JNK1 and JNK2 are widely expressed in many tissues, but JNK3 is expressed predominantly in nervous system. Mice deficient in the single gene of *Jnk1*, *Jnk2*, or *Jnk3*, and *Jnk1*/*Jnk3*– or *Jnk2*/*Jnk3*–double mutant mice all survived normally. Mice lacking both JNK1 and JNK2 die around embryonic day 11 (E11) with severe dysregulation of apoptosis in the brain (*7*, *8*). Specifically, there was a reduction of cell death in the lateral edges of the hindbrain prior to neural tube closure. In contrast, increased apoptosis and caspase activation were found in the mutant forebrain. These results assign both pro-and anti-apoptotic functions to JNK1 and JNK2 in the development of the fetal brain.

Sek1$^{-/-}$ embryos die between E10.5 and E12.5 with impaired liver formation and massive apoptosis (*9–12*). We have recently shown that SEK1-mediated SAPK/JNK pathway downstream TNF-α receptor 1 (TNFR1) participates in embryonic hepatoblast proliferation and survival via a pathway different from NF-κB–induced anti-apoptosis (*13*). Furthermore, *mkk7*$^{-/-}$ embryos die between E11.5 and E12.5 with similar defects in liver formation (*14*). These results indicate that SEK1 and MKK7 cannot substitute for one another *in vivo* and that both are important for hepatoblast proliferation and survival during mouse embryogenesis (Fig. 1).

Role of SAPK/JNK in apoptosis regulation

It has been proposed that SAPK/JNK activation triggers the mitochondria-dependent apoptosis in response to many types of stress, including UV-irradiation. Both *Jnk1*$^{-/-}$ *Jnk2*$^{-/-}$ and *sek1*$^{-/-}$ *mkk7*$^{-/-}$ mouse embryonic fibroblasts (MEFs) exhibited profound defects in stress-induced apoptosis (*15*, *16*). These results strongly suggest that the SAPK/JNK activation directly regulates mitochondria-dependent apoptosis in the pro-apoptotic direction. In contrast, *sek1*$^{-/-}$ *mkk7*$^{-/-}$ ES cells show normal apoptotic responses, including DNA fragmentation and